nature ecology & evolution

Article

https://doi.org/10.1038/s41559-026-03044-y

Direct benefits are not necessary for the evolution of multicellularity

Received: 10 July 2025

Accepted: 4 March 2026

Published online: 20 April 2026

Check for updates

Daniel Jorge[1,4], Merlijn Staps[1,4], Yuriy Pichugin[1,2,4] & Corina E. Tarnita[1,3]

The evolution of multicellularity required nascent multicellular life to persist in a unicellular world. Because grouping usually comes with steep costs, multicellularity had to confer some benefits. While direct benefits—in which cells in groups outperform single cells under the same conditions—can clearly suffice for multicellularity to evolve, whether they were also necessary has not been systematically explored. Here we develop a general model for the evolution of multicellularity in a spatially heterogeneous environment and show that direct benefits are, in fact, not necessary. When nascent multicellular groups differ from their unicellular ancestor in their spatial distribution (for example, because groups sink), two distinct indirect benefits can emerge: escape from competition from the unicellular ancestor and increased exploitation of desirable environments. Either benefit can drive the evolution of multicellularity in the absence of direct benefits. As a case study, we show that in the Proterozoic Ocean, where several multicellular eukaryotic lineages originated, escape from competition could have driven the evolution of multicellularity by offsetting the costs of diffusion limitation and oxygen deprivation. Our work systematically uncovers hitherto underappreciated mechanisms by which multicellularity can evolve, even under seemingly adverse conditions, and highlights the importance of ecology in explaining major evolutionary transitions.

All multicellular life has evolved from unicellular ancestors through a number of independent evolutionary transitions[1–6]. These evolutionary transitions required nascent multicellular organisms to persist—and eventually thrive—in a unicellular world. There is no reason to believe that this was an easy feat. Let us ponder, for instance, the evolution of multicellularity in the Proterozoic Ocean, the largely oxygen-deprived marine environment where the first multicellular red and green algae as well as the ancestors of animals originated at some point during the Proterozoic Eon (2,500 to 543 million years ago)[4,7–14]. In this environment, groups might have paid oxygen-diffusion costs with increasing size[9,15–17]. Moreover, groups might also have sunk to lower layers of the water column (for example, due to the loss of active movement[18–20] and/or increased sedimentation rates[2,16,21–24]), which are thought to have been even more deprived of oxygen at that time[8,10,25,26]. In light of these challenges—oxygen-diffusion limitation and possibly sinking to even more oxygen-deprived lower layers—it would appear that the decks were stacked against multicellularity, and one would naively expect that any multicellular mutant would perish in competition with its unicellular ancestor.

That grouping comes with potentially steep costs, especially stemming from nutrient access limitation, has been recognized broadly across the study of the multiple origins of multicellularity[27–30]. Multicellularity would only be able to evolve if some benefits were to offset these costs. And indeed, multicellularity could provide various benefits that give cells in groups a net growth rate advantage over single cells (reviewed in refs. 23,31), either by increasing their birth rate (for example, via division of labour between cells or improved extracellular metabolism) or by improving their survival (for example, via predator

[1]Department of Ecology and Evolutionary Biology, Princeton University, Princeton, NJ, USA. [2]Department of Theoretical Biology, Max Planck Institute for Evolutionary Biology, Plön, Germany. [3]Collegium Helveticum, Zürich, Switzerland. [4]These authors contributed equally: Daniel Jorge, Merlijn Staps, Yuriy Pichugin. e-mail: ctarnita@princeton.edu

https://doi.org/10.1038/s41559-026-03044-y

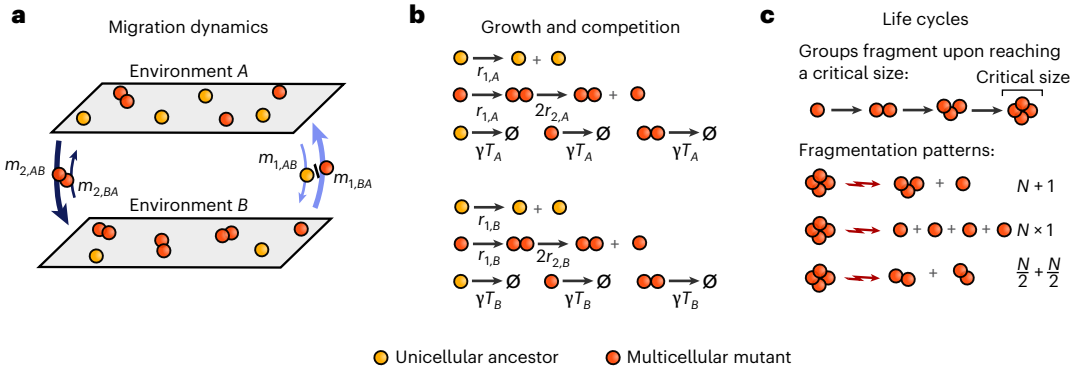

Fig. 1 | Model overview. a, We model competition between a unicellular ancestor (life cycle 1 + 1, grey) and a multicellular mutant (here shown as the simplest possible life cycle, 2 + 1, in red). Cells and groups migrate between two environments; competition occurs locally. The one-cell stage of the multicellular mutant is subject to the same migration rates ($m_{1,AB}$ and $m_{1,BA}$) as the unicellular ancestor. Groups of size n migrate at rates $m_{n,AB}$ and $m_{n,BA}$, as indicated by the dark blue arrows for $n = 2$. **b**, Cell division rates ($r_{n,A}$ and $r_{n,B}$) depend on the environment (A or B) and the group size ($n \geq 1$). For the unicellular ancestor, cells separate upon division. For the multicellular mutant (here shown as 2 + 1), cells remain attached until a critical size is reached, upon which the group instantaneously fragments (see **c**). All life stages are subject to density-dependent death due to competition within their environment; T_A and T_B denote the total density of cells in each environment, and γ is the competition rate. **c**, We consider three different life cycles that differ in how they fragment: production of one single-celled propagule ($N + 1$ life cycle), dissolution into solitary cells ($N \times 1$ life cycle) or splitting into two groups of equal size ($N/2 + N/2$ life cycle). Here we show 3 + 1, 4 × 1 and 2 + 2 as examples. See Methods for the detailed model description.

avoidance or resistance to environmental stress). We refer to such advantages, in which cells in groups outperform solitary cells under the same conditions, as direct benefits.

While complex multicellular organisms clearly reap various direct benefits of multicellularity, it is unknown whether such benefits were present at the origins of multicellularity. Especially for those direct benefits that require coordination among cells (for example, controlled cell differentiation), it seems unlikely (although not necessarily impossible[32–34]) that they would have emerged immediately at the onset of grouping. Recognizing this problem, some authors have proposed that, initially, multicellularity might have been neutral at best: perhaps multicellular groups 'initially had neither advantage nor disadvantage and survived by drift until some further mutational change endowed them with a skill that was not possible for their single-cell relatives'[1].

The intuition that the evolution of multicellularity would have required direct benefits stems from the idea of competitive exclusion: if cells in groups are at a net growth rate disadvantage compared to solitary cells, then any multicellular mutant would necessarily be outcompeted by the unicellular ancestor. However, this competitive-exclusion framing implicitly assumes that the ecological niche of nascent multicellular groups perfectly overlaps with that of their unicellular ancestor and, in particular, that they use space in the same way. In reality, the spatial distribution of emergent groups could differ from that of single cells, for example, due to sinking[2,16,21–24,35], improved adhesion[5,36], faster/slower locomotion[18,20,37] or improved chemotaxis[38,39]. The resulting spatial heterogeneity between solitary cells and multicellular groups complicates the ecological dynamics and raises the question whether differential use of space could immediately confer some indirect benefits and whether those benefits could drive the evolution of multicellularity even when there are costs to forming groups. Here we develop a general framework to systematically investigate these questions.

Results

Spatial heterogeneity can drive the evolution of multicellularity through indirect benefits

We consider the simplest spatial setting that allows us to explore the possibility of indirect benefits: two environments, A and B, with possibly different growth conditions and linked by migration (Fig. 1a,b). These could be, for instance, different water layers, different substrates, or water and a liquid-surface interface. We compete a resident unicellular strategy against an invading multicellular strategy; for the latter, we explore several different life cycles (Fig. 1c). For a detailed model description, see Methods. To reflect the premise of no direct benefit, we assume that, regardless of environment, single cells have a higher intrinsic growth rate than cells in groups of size $n > 1$, that is, $r_{n,A} < r_{1,A}$ and $r_{n,B} < r_{1,B}$. Under this assumption, multicellularity cannot evolve if cells are restricted to a single environment (Supplementary Information section 2.4), confirming the intuition that direct benefits are needed in the absence of spatial heterogeneity.

To investigate whether and when multicellularity can evolve in this two-environment setting, we characterize both the short-term fate of a multicellular mutant arising in a stable resident unicellular population (that is, does it invade or does it go extinct?) and the long-term outcome of an invasion (that is, does the mutant displace or coexist with the ancestor?). We analytically derived a mathematical condition for a multicellular mutant to be able to invade from rare (Supplementary Information section 2.3), which we complemented with numerical simulations to determine the long-term outcome.

The invasion analysis captures the differences in performance between groups and single cells via two fundamental quantities, R_n and C_n, where

$$R_n = \frac{p_{n,A} r_{n,A} + p_{n,B} r_{n,B}}{q_A r_{1,A} + q_B r_{1,B}} \quad (1)$$

is the average growth rate of cells in groups of size n, relative to the growth rate of the ancestor, and

$$C_n = \frac{p_{n,A} q_A + p_{n,B} q_B}{q_A^2 + q_B^2} \quad (2)$$

is the average amount of competition from ancestral cells experienced by cells in groups of size n, relative to the amount of competition experienced by the ancestor from itself. Here q_A and $p_{n,A}$ are the fractions of ancestral solitary cells, respectively multicellular life stages of size $n \geq 1$, that inhabit environment A during the invasion from rare (see Methods); the remaining fractions $q_B = 1 - q_A$ and $p_{n,B} = 1 - p_{n,A}$ inhabit environment B.

We can interpret R_n/C_n as the basic reproduction number of cells in groups of size $n \geq 1$ (Supplementary Information section 2.3): cells in groups of size n perform better than the unicellular ancestor when $R_n/C_n > 1$. The necessary and sufficient condition for multicellularity

https://doi.org/10.1038/s41559-026-03044-y

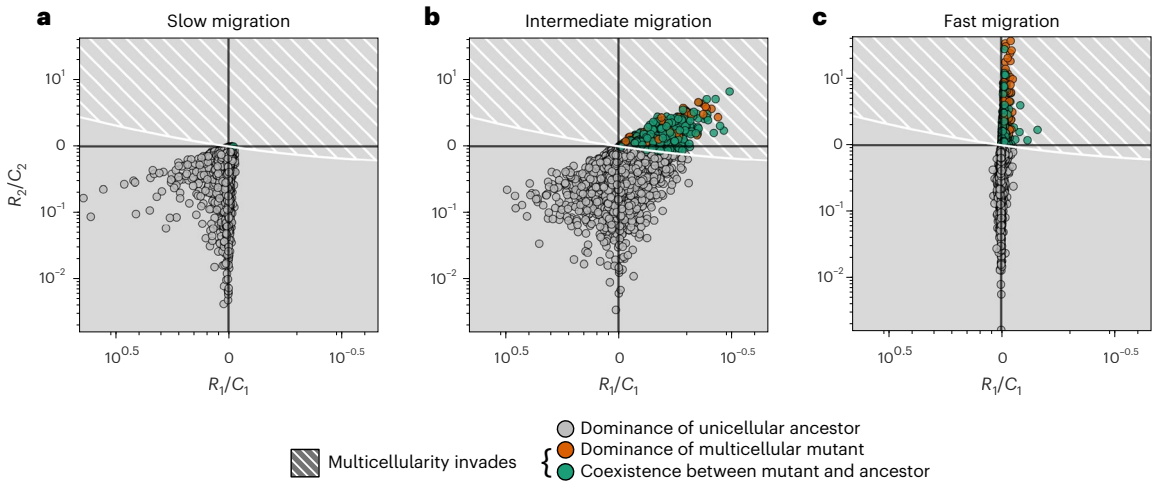

Fig. 2 | Spatial heterogeneity can drive the evolution of multicellularity through indirect benefits. Evolutionary outcomes for the 2 + 1 life cycle for randomly sampled migration rates $m_{1,AB}$, $m_{1,BA}$, $m_{2,AB}$ and $m_{2,BA}$, and reproduction rates $r_{1,A}$, $r_{1,B}$, $r_{2,A}$ and $r_{2,B}$ (subject to $r_{1,A} > r_{2,A}$ and $r_{1,B} > r_{2,B}$, that is, no direct benefits). The long-term outcomes (specified by the colour of the points) were determined by numerically simulating the dynamics of a rare 2 + 1 life cycle mutant introduced into a stable resident unicellular population. The location of each data point in $(R_1/C_1, R_2/C_2)$ space was found by numerically evaluating q_A, q_B, $p_{1,A}$ and $p_{1,B}$, $p_{2,A}$ and $p_{2,B}$ for a rare multicellular invader at the unicellular ancestor's steady state (see Methods for details). The long-term simulations confirm that the 2 + 1 life cycle successfully invades (leading to dominance or coexistence) in—and only in—the hatched region, whose boundary is given by the analytically derived equation (3). All simulations led to a stable steady state (no oscillations were observed). In all panels, the vertical black lines indicate where $R_1/C_1 = 1$; the horizontal black lines indicate where $R_2/C_2 = 1$. No simulated points fell to the left of the $R_1/C_1 = 1$ line, and we confirmed this analytically (Supplementary Information section 2.4). **a**, Results for slow migration, $M/R = 0.02$. **b**, Results for intermediate migration, $M/R = 1$. **c**, Results for fast migration, $M/R = 50$. Here, $M = m_{1,AB} + m_{1,BA} + m_{2,AB} + m_{2,BA}$ is the total migration rate and $R = r_{1,A} + r_{1,B} + r_{2,A} + r_{2,B}$.

to invade from rare is a complicated expression that depends on the values of R_n/C_n across all stages $n = 1, 2, \ldots, N$ of the multicellular life cycle (equation (12) in the Methods) and thereby on the emergent spatial distribution of multicellular groups of different sizes. But, for the simplest multicellular life cycle, 2 + 1, this necessary and sufficient condition is simple enough to explore further:

$$\frac{R_1}{C_1} \cdot \left(2 \cdot \frac{R_2}{C_2} - 1\right) > 1. \quad (3)$$

To determine whether inequality (3) can be satisfied in the absence of direct benefits, we evaluated R_1, R_2, C_1 and C_2 for a large number of randomly sampled growth rates $r_{1,A}$, $r_{2,A}$, $r_{1,B}$, $r_{2,B}$ (subject to $r_{1,A} > r_{2,A}$ and $r_{1,B} > r_{2,B}$) and migration rates $m_{1,AB}$, $m_{1,BA}$, $m_{2,AB}$, $m_{2,BA}$ (Methods). We found that multicellularity can indeed evolve in the absence of direct benefits: many sampled parameter sets fell inside the analytically derived hatched region in Fig. 2, where the invasion condition (3) holds. Moreover, we numerically simulated the invasion of a 2 + 1 multicellular mutant for each sampled parameter set, and in all cases the simulated invasion outcomes matched those predicted by (3), thereby confirming the analytical results.

While there are many combinations of parameters for which multicellularity invades, the results depend strongly on the timescale of migration relative to the timescale of reproduction. When migration is much slower than reproduction, multicellularity fails to invade (Fig. 2a; almost all points land outside the hatched region). Intuitively, this makes sense as in the limit of very slow migration we recover the case of isolated environments where the local growth disadvantage of multicellularity leads to competitive exclusion.

When migration and reproduction occur on similar timescales (Fig. 2b), the spatial distributions of the three populations of interest (the ancestral solitary cells and the one-cell and two-cell stages of the multicellular invader) can deviate substantially. As a result, it is now possible for multicellularity to invade. This can happen because of indirect benefits to both the one-cell and two-cell stages of the multicellular life cycle (upper right quadrant) but, interestingly, also via indirect benefits to the one-cell stage alone (that is, $R_1/C_1 > 1$ but $R_2/C_2 < 1$; hatched region in the lower right quadrant).

Finally, when migration is much faster than reproduction (Fig. 2c), the one-cell stage of the multicellular strategy reaches essentially the same spatial distribution as the unicellular ancestor and, as a result, has very similar performance ($R_1/C_1 \approx 1$; note that the points in Fig. 2c approach the vertical black line). However, the spatial distribution of two-cell groups can still be different, allowing cells in two-cell groups to enjoy indirect benefits ($R_2/C_2 > 1$) that lead to the invasion of multicellularity.

Altogether, we conclude that indirect benefits can indeed lead to the invasion of multicellularity for a broad range of parameters, provided that migration between the different environments occurs sufficiently quickly relative to the timescale of reproduction. The outcome of the invasion can be either coexistence with or displacement of the ancestor (Fig. 2).

There are two kinds of indirect benefits: escaping competition and environmental exploitation

To better understand how spatial heterogeneity confers indirect benefits, we first focus on the special case of the 2 + 1 life cycle in the limit of fast migration. In this extreme case, as we saw above, $R_1/C_1 = 1$, and condition (3) simplifies such that multicellularity can invade from rare if and only if

$$R_2 > C_2. \quad (4)$$

Thus, indirect benefits must arise in the two-cell stage of the multicellular life cycle. These indirect benefits can arise in two non-mutually exclusive ways: a reduction in the amount of competition experienced ($C_2 < 1$) and/or an increase in the average growth rate ($R_2 > 1$).

First, if the distribution of single cells is biased towards one of the two environments, cells in two-cell groups can escape competition from single cells if groups are biased towards the other environment or towards the same environment but less strongly ($C_2 < 1$; blue and purple regions in Fig. 3a). An example of escaping competition

https://doi.org/10.1038/s41559-026-03044-y

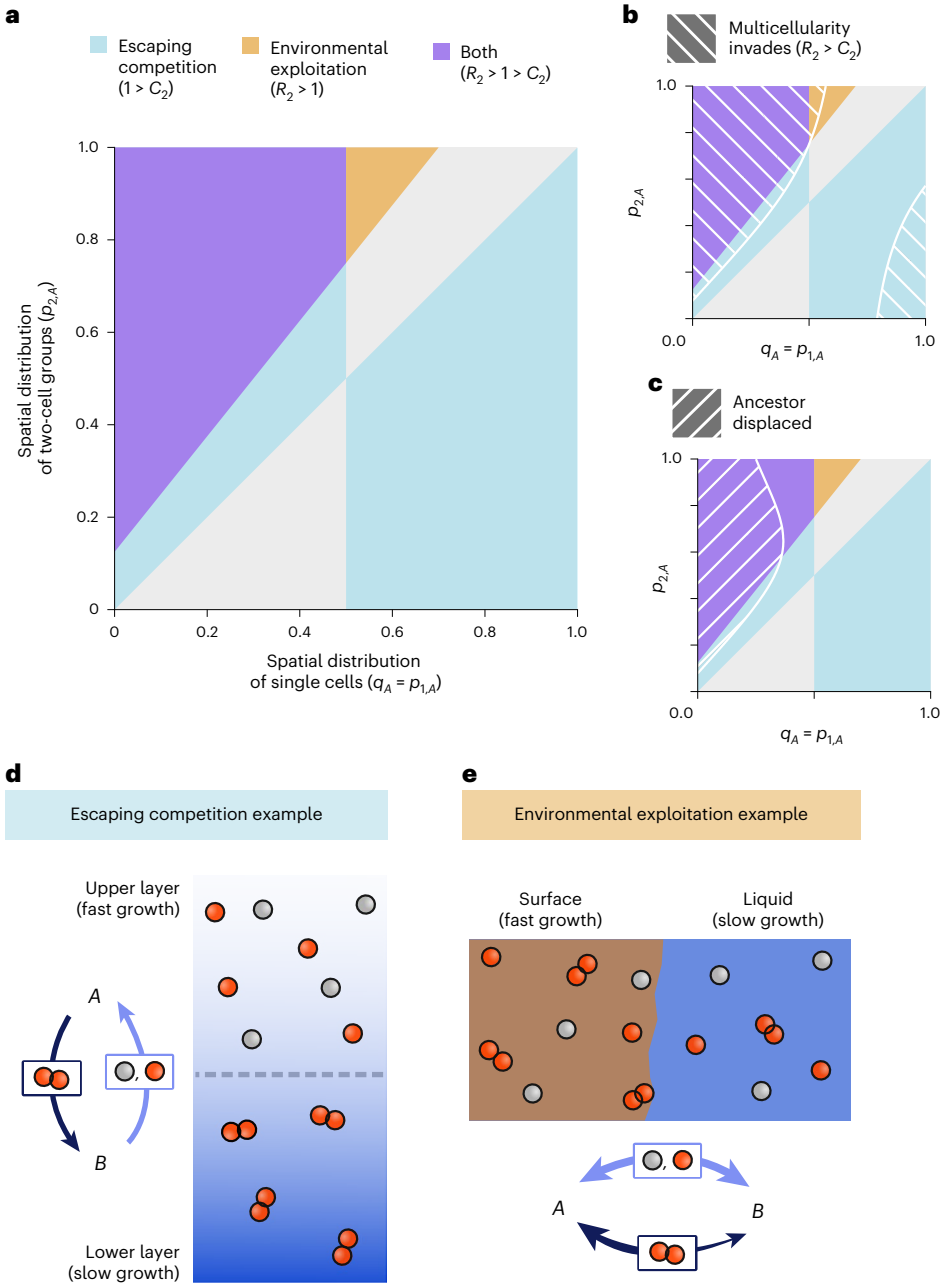

Fig. 3 | Multicellularity can evolve via escaping competition, environmental exploitation or both. a, Possible indirect benefits and invasion outcomes in the fast migration limit, depending on the steady-state proportion of single cells ($q_A = p_{1,A}$) and two-cell groups ($p_{2,A}$) in environment A. As here we assume fast migration (which implies $R_1 = C_1$) the classification of indirect benefits depends solely on $R_2 = (p_{2,A}r_{2,A} + p_{2,B}r_{2,B})/(q_A r_{1,A} + q_B r_{1,B})$ and $C_2 = (q_A p_{2,A} + q_B p_{2,B})/(q_A^2 + q_B^2)$, where the spatial distributions of single cells and groups are completely determined by the migration rates; see equations (5) and (6) in the Methods. Parameters: $r_{1,A} = 15$, $r_{2,A} = 12$, $r_{1,B} = 5$, $r_{2,B} = 4$, so that growth rates are 3 times higher in environment A than in environment B and cells in groups have a 20% reduction in growth rate relative to single cells in both environments. **b**, Region where indirect benefits are strong enough to lead to the invasion of multicellularity ($R_2 > C_2$). **c**, Subset of the region in **b** where the multicellular mutant eventually displaces (rather than coexists with) the unicellular ancestor, as determined by numerical simulation. **d**, When groups sink to a resource-poor lower layer ($p_{2,A} = 0$) and solitary cells rise to a resource-rich upper layer ($q_A = p_{1,A} = 1$), multicellularity can invade through escaping competition as long as cells have a positive growth rate in the lower layer ($r_{2,B} > 0$). **e**, When solitary cells are equally distributed between a resource-rich surface and a resource-poor liquid ($q_A = p_{1,A} = 0.5$), multicellularity can invade through environmental exploitation as long as the spatial distribution of groups is sufficiently biased towards the surface ($p_{2,A} > 0.75$ for the parameters in **a**).

arises in an aquatic environment if groups sink to lower layers with a low density of single cells, even if those lower layers are largely deprived of resources. For instance, in the extreme case where solitary cells are completely restricted to the upper layer and groups are completely restricted to the lower layer (Fig. 3d), multicellularity can invade as long as cells in groups are able to divide in the lower layer, even if the rate at which they do so is much lower than in the upper layer.

Second, if the spatial distribution of two-cell groups is biased towards the environment with a higher r_2 (in Fig. 3a, this is environment A), then, on the whole, cells in groups can experience a higher average growth rate than single cells ($R_2 > 1$; orange and purple regions in Fig. 3a)

despite having a lower growth rate in either environment. This is an example of Simpson's paradox, the statistical phenomenon that a trend that exists across different populations (that is, groups have a lower growth rate in both environments) may reverse when the populations are combined (that is, groups have a higher average growth rate across the environments). We call this second pathway environmental exploitation. An example of environmental exploitation can arise if groups are better than solitary cells at adhering to a surface (Fig. 3e), which could be desirable if the surface has more resources or protects from predators or environmental stress. Even if solitary cells are equally distributed between the surface and the liquid—making it impossible to escape competition from them—multicellularity can invade through environmental exploitation as long as the spatial distribution of groups is sufficiently strongly biased towards the surface.

Both escaping competition and environmental exploitation can drive the invasion of multicellularity on their own (hatched blue and hatched orange regions in Fig. 3b) if they confer a sufficiently strong indirect benefit. The pathways may also act simultaneously, in which case multicellularity automatically invades (hatched purple region in Fig. 3b) because $C_2 < 1$ and $R_2 > 1$ together imply $R_2 > C_2$. Conversely, when cells in groups are neither able to escape competition nor to exploit the environment (grey region in Fig. 3a), then multicellularity can never invade because $C_2 \geq 1$ and $R_2 \leq 1$ together imply $R_2 \leq C_2$ (Fig. 3b). In terms of long-term outcome (Fig. 3c), simulations show, as before, that when multicellularity invades, it either eventually displaces the unicellular ancestor or stably coexists with it. The outcome, however, is not exclusively determined by the underlying pathway: both escape from competition and environmental exploitation can lead to both possible outcomes depending on the parameters (in particular, although it does not occur for the parameters in Fig. 3, the unicellular ancestor can also be displaced when only environmental exploitation occurs; Extended Data Fig. 1).

The intuition behind the two pathways extends beyond the choice of the 2 + 1 life cycle and the fast migration limit. In particular, multicellularity can only invade if at least one stage $n \geq 1$ of the life cycle satisfies $R_n/C_n > 1$ (Supplementary Information section 2.4), which can be broken down into the same three alternatives discussed above: escape from competition ($1 > C_n$), environmental exploitation ($R_n > 1$) or both. In other words, a necessary (but in general not sufficient) condition for the invasion of multicellularity in the absence of direct benefits is that at least one life stage of the multicellular life cycle offers indirect benefits through escape from competition or environmental exploitation.

The evolution of indirectly beneficial multicellularity can lead to diverse ecological outcomes

Finally, we investigate what stable ecological communities of unicellular and/or multicellular life cycles might arise in an evolutionary process where multicellular life cycles of different sizes can continuously arise via mutation. In this broader setting, we can also probe what group sizes will be selected for.

To constrain the scope of this broad question, we return to the example that motivated our theoretical inquiry into indirect benefits—the Proterozoic Ocean, where several multicellular lineages originated, such as animals and the first red and green algae[7,9,12,13,40]. While much remains unclear about the unicellular ancestors of these lineages and their ecology, it is plausible that at least some were (a) facultative aerobes, able to perform both respiration and fermentation (which was likely the case for animals[9,41] and might have even been the ancestral state of all eukaryotes[9,41–43]), and (b) planktonic, making use of oxygen that was primarily available in the upper layers of the Proterozoic Ocean[9,10,44–46]. Starting from such a planktonic, facultatively aerobic ancestor, a mutant capable of group formation could have been subjected to downward movement to lower layers of the water column (as observed in the lab[21,22,47–49] and thought to occur in marine ecosystems[21,23,50,51]), as well as to oxygen deprivation, as cells in the interior of the multicellular group would have had limited access to oxygen[15,52]. In the modern atmosphere, the depth of oxygen penetration into living tissues is about 1 mm, but, in the Proterozoic, oxygen levels were much lower, especially at depth, so oxygen deprivation should have kicked in at small group sizes[8,17,25,53].

To minimally capture the above scenario, we assume perfect spatial segregation (Fig. 4a): single cells and groups smaller than a critical size, N_S, inhabit the upper layer, owing to buoyancy or active taxis; groups of size equal to or larger than the critical size sink and inhabit the lower layer, owing to loss of buoyancy or inability to coordinate taxis; when cells or groups smaller than the sinking size N_S are produced by fragmentation in the lower layer, they instantaneously rise up to the upper layer. Subsequently, we relax this perfect segregation assumption and allow for various degrees of mixing between the layers (Supplementary Information section 3.6). To model oxygen availability, we introduce two control parameters, N_U and N_L, which set the maximum size groups can grow to in the upper and lower layers before oxygen deprivation kicks in. In both layers, cells up to this maximum size have access to oxygen and divide at a rate r_o; additional cells are restricted to fermentation and divide at a lower rate r_f (Fig. 4a; Methods). The critical group sizes N_U and N_L reflect both the concentration of dissolved oxygen in the corresponding layer and the metabolic and biophysical properties of nascent multicellular groups (for example, denser clusters may face limitations at smaller group sizes than more branched or filamentous forms). For simplicity, we do not consider additional costs associated with increasing group size beyond oxygen-diffusion limitation, but we reflect on this assumption as we discuss our results.

Throughout the Proterozoic Eon, atmospheric oxygen levels increased, and, consequently, so did oceanic oxygen; however, the exact dynamics of this rise remain unclear[10,53]. Furthermore, lower-layer oxygen availability might have depended on oceanic depth—for example, marine shelves might have been more oxygenated than the deep ocean[10,25]. Therefore, we arbitrarily vary N_U and N_L, subject to the constraint $N_L \leq N_U$, to capture a range of plausible scenarios, including earlier (N_U, N_L low) versus later (N_U, N_L high) during the Proterozoic, and shallower ($N_U - N_L$ smaller) versus deeper ($N_U - N_L$ higher) oceans.

To simulate the evolutionary process, we start from the unicellular ancestor and allow any life cycle of the form $N + 1$ to arise by mutation and compete (Fig. 4b). We assume that mutations are rare and, thus, only introduce a new mutant when the ecological dynamics involving the previous mutant have stabilized. We continue the simulation until a community emerges that cannot be invaded by any other life cycle, that is, an evolutionarily stable community (ESC)[54,55]. We find four qualitatively different ESC regimes (Fig. 4c,d). Typically, one multicellular life cycle is present, either subject to directional selection for increased size (regime I) or stabilizing selection for an intermediate size (regimes II and III); regime IV is an exception in which all life cycles up to a given size coexist. The regimes also differ in the fate of the unicellular ancestor. In the Supplementary Information, we provide a detailed classification of the regimes (Supplementary Information section 3.5), complemented by an exhaustive mathematical analysis (Supplementary Information section 4); here we focus on the main patterns that arise.

What group sizes evolve depends on oxygen availability across the two layers (and thus N_U and N_L; Fig. 5a,b), which sets the trade-off between the benefits and costs of group formation. The largest groups evolve at either very low or very high oxygen availability (Fig. 5c). When oxygen is either abundant (sufficiently high N_U and N_L) or entirely absent ($N_U = N_L = 0$), group-formation costs are negligible and groups can grow large without penalty (regime IV). When oxygen is present but scarce (low N_U and N_L, but $N_U > 0$), group-formation costs are steep, leaving groups at a strong competitive disadvantage against the unicellular ancestor in the upper layer; so, selection favours large group sizes because they can more effectively escape upper-layer competition (regime I). By contrast, at intermediate oxygen concentrations, selection favours intermediate group sizes (Fig. 5c, regimes II and III):

https://doi.org/10.1038/s41559-026-03044-y

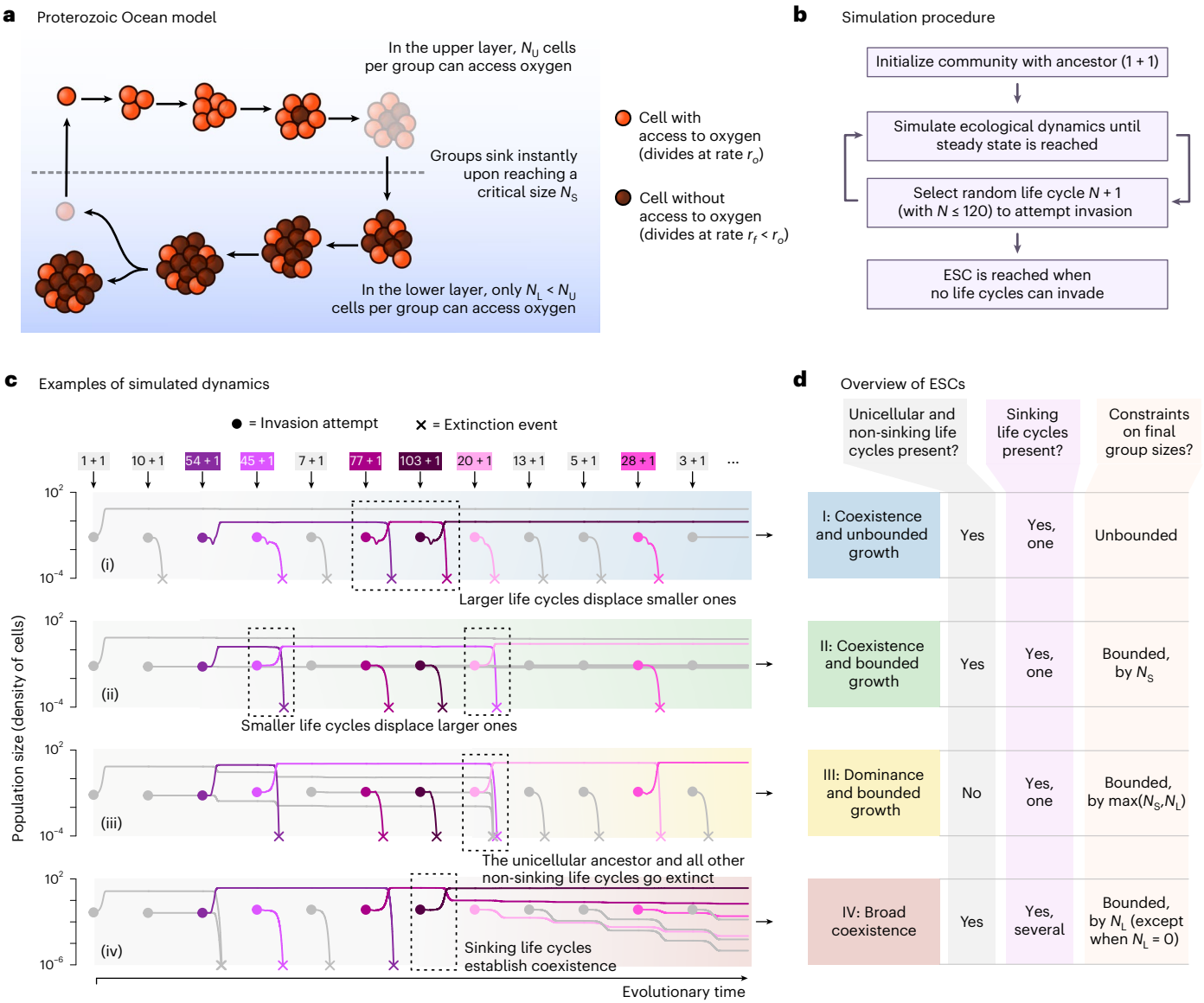

Fig. 4 | Diverse evolutionary outcomes in a model of indirectly beneficial multicellularity in the Proterozoic Ocean. a, We assume that cells up to a critical size have access to oxygen and divide at a higher rate. The critical size differs between the upper and lower layer (separated by the dashed line); in the schematic, we have $N_U = 6$, $N_L = 4$, $N_S = 9$. **b**, Procedure to determine ESCs; see main text and Methods for details. **c**, Examples of evolutionary dynamics for $N_S = 20$ and $(N_U, N_L) = (4, 2)$ (i), (18, 2) (ii), (120, 28) (iii) and (120, 120) (iv), giving rise to four qualitatively different types of ESCs. Invading mutant life cycles (indicated by arrows) are coloured by their fragmentation size. For illustrative purposes, we show the same sequence of invasion attempts for all four examples; in the actual simulations, mutants are drawn at random. Enough mutations are shown to reach a community that has the same structure as the ultimate ESC. **d**, Categorization of qualitatively different ESC outcomes. Sinking life cycles are those that reach size at least N_S. Non-sinking life cycles that avoid oxygen deprivation ($N \leq N_U$ and $N < N_S$) are neutral with respect to the ancestor and thus share its fate: they are present in the ESC when the ancestor is, and absent when it is not.

large enough to sink and escape competition, yet small enough to avoid substantial oxygen deprivation.

The fate of the unicellular ancestor depends on the group sizes that evolve. Life cycles with sufficiently large groups mostly occupy the lower layer, leading to coexistence with the ancestor via niche partitioning (regimes I and IV; Fig. 4c). Intermediate-sized groups, by contrast, can lead to either coexistence (Fig. 4c, regime II) or displacement of the ancestor (Fig. 4c, regime III), depending on oxygen availability (Fig. 5a,b). Interestingly, intermediate-sized groups can also displace the ancestor at the extremes of oxygen availability (regime IV; Fig. 4c), but there the displacement is only temporary: the ancestor becomes able to re-invade once sufficiently large groups emerge. At this point, broad coexistence of all life cycles up to a given size establishes (Supplementary Information section 4.4).

In summary, our exploration of indirectly beneficial multicellularity in the Proterozoic Ocean reveals a diversity of ecological outcomes and a non-monotonic relationship between evolved group size and oxygen availability. An extensive analysis shows that these qualitative results are robust to relaxing specific assumptions of our implementation, including the type of multicellular life cycle (Extended Data Fig. 2), the relative benefits of oxygen r_o/r_f (Extended Data Figs. 3 and 4) and the perfect spatial segregation between upper and lower layers (Extended Data Fig. 5).

Discussion

What selective factors drove the evolution of multicellular life is a long-standing open question[56–58]. Here we have introduced a new way to organize the various benefits that have been proposed: we distinguish

https://doi.org/10.1038/s41559-026-03044-y

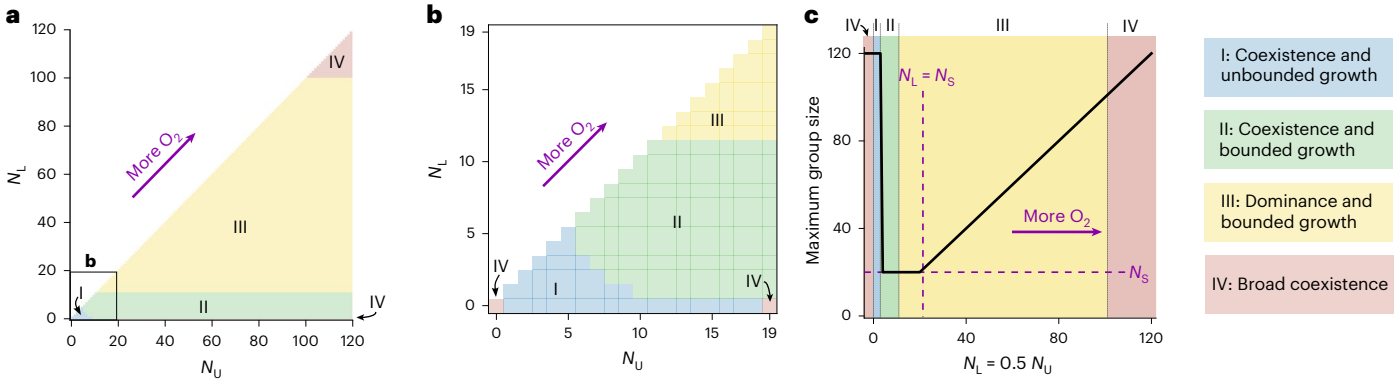

Fig. 5 | Evolutionary outcomes are shaped by oxygen availability. **a**, ESC outcomes as a function of the oxygen availability in the upper layer (N_U) and lower layer (N_L), for a sinking size $N_S = 20$. Regimes I–IV are the same as in Fig. 4d. When $N_U \geq N_S - 1$, the value of N_U becomes irrelevant as all cells in the upper layer have access to oxygen. **b**, A zoom in on the ESC outcomes for $N_U < N_S$. **c**, Maximum attained group sizes as a function of oxygen concentration, under the assumption that $N_U = 2N_L$. Background colours indicate the ESC reached for each given N_L. Simulations used $r_o = 6.8$ and $r_f = 1$, following a recent empirical study[15] (but see Extended Data Figs. 3 and 4 for other values of r_f/r_o).

between direct benefits (for example, release from phagotrophic predation, improved stress resistance, division of labour) which yield some advantage to groups relative to single cells in the same local environment, and indirect benefits, which offer no local advantage to groups but emerge at the population level as a consequence of the average environment experienced by groups. The key distinction is that indirect benefits require spatial heterogeneity and differential space use between unicellular and multicellular strategies, whereas direct benefits can arise even in homogeneous environments. We show that two kinds of indirect benefits are possible—environmental exploitation and escaping competition—and that both are able to drive the evolution of multicellularity even in the absence of any direct benefits, that is, under adverse conditions in which multicellularity is selected against in each individual environment.

The first indirect benefit, environmental exploitation, refers to situations in which groups have improved access to a desirable environment, even though, in this desirable environment, they still perform worse than solitary cells. This potential benefit of multicellularity has been recognized across a range of different scenarios: in an aquatic environment, groups may sink to lower layers devoid of predators or pathogens[23], groups may attach to a surface where they cannot be swept away by currents[5,36,59], or groups may have improved chemotaxis and be better at finding patches with resources[38,39]. There is less precedent for the second indirect benefit, release from competition with the unicellular ancestor (but see ref. 60), which depends not on the quality of an environment but on the extent to which the unicellular competitor occupies it. Escaping competition is intrinsically less intuitive, because it can apply even when groups are biased towards less desirable environments. For example, in the Proterozoic Ocean, sinking to lower layers could have allowed multicellularity to evolve despite groups facing a double cost of increased diffusion limitation and exclusion from oxygen, which was mostly restricted to the upper layer[9,10,45,46].

Our finding that spatial heterogeneity can allow a multicellular mutant to persist, even when faced with competition from the unicellular ancestor, comports with the general ecological idea that spatial heterogeneity can support coexistence[61–64]. In particular, our model evokes the notion of a competition–colonization trade-off[65–67], as an inferior competitor (the multicellular mutant) is able to persist thanks to spatial heterogeneity. However, while competition–colonization models predict either coexistence or exclusion of the inferior competitor, in our model, the superior competitor (the unicellular ancestor) can end up being excluded by the inferior competitor (the multicellular mutant). This type of outcome is more consistent with ecological models where different life stages inhabit different environments, which have been built to study the dynamics of species with complex life cycles (for example, frogs where the tadpole is aquatic but the adult is terrestrial)[68–70].

Our in-depth exploration of indirectly beneficial multicellularity in the Proterozoic Ocean uncovered a diversity of ecological outcomes and a non-monotonic relationship between group sizes and oxygen availability. Large group sizes evolve when there is either little oxygen (and all or almost all cells are restricted to fermentation) or abundant oxygen (when all or almost all cells can access oxygen), which generally leads to coexistence between unicellular and multicellular strategies. By contrast, at intermediate oxygen concentrations, selection favours intermediate group sizes: large enough to sink, yet small enough to avoid substantial oxygen deprivation. This generally results in the exclusion of the unicellular ancestor, because the smaller stages of the multicellular strategy still exert a strong competitive pressure on the upper layer. Of course, all these results assume the existence of an oxygen-mediated trade-off, which may not exist for some multicellular forms (for example, some filaments).

This non-monotonic relationship may have implications for the timing of multicellular origins across major eukaryotic lineages, which are typically thought to have arisen only towards the end of the Proterozoic[9,12–14], despite some apparent, but controversial, deeper time fossil evidence of macroscopic multicellularity[40,71–74]. Our finding that large groups evolve at low oxygen concentrations suggests that macroscopic multicellularity could, actually, have evolved earlier in the Proterozoic. However, if macroscopic multicellularity did, indeed, evolve in the early Proterozoic, our model also predicts that it would have gone extinct, displaced by smaller multicellular forms, as oxygen levels continued to increase. But this displacement would have been possible only if the larger multicellular forms did not evolve—for lack of time or metabolic/biophysical capabilities—additional benefits of group living that could have offset the oxygen-mediated trade-off.

A detailed comparison is worth making between the results of our Proterozoic Ocean model and empirical work in snowflake yeast. Multicellular snowflake yeast evolves in experiments where unicellular yeast is exposed to selection for fast growth (favouring single cells and smaller groups that minimize oxygen deprivation) and selection for settling (favouring larger groups that sink faster)[22]. Thus, much like our set-up, this system features a size-dependent trade-off between the benefits and costs of multicellularity. But it fundamentally differs from our set-up because the benefits of multicellularity are direct rather than indirect. Nonetheless, empirical work on snowflake yeast has also revealed suppression of group size

at intermediate oxygen concentrations[15]. This convergence in findings reinforces the robustness of the non-monotonicity and can be explained from the size-dependent trade-off, which exists in both the indirect and direct settings and is most pronounced at intermediate oxygen concentrations.

Altogether, our results make a theoretical case for indirect benefits as a worthwhile research avenue. But is there evidence that they exist in reality? Lab experiments that explicitly incorporate spatial heterogeneity provide some promising examples. For instance, in spatially structured experimental microcosms, *Pseudomonas fluorescens* bacteria evolve to form sticky multicellular mats that take advantage of a high-oxygen air–liquid interface[75–78]. The glue necessary to form and maintain the mat is costly, giving the multicellular mutants an intrinsic growth rate disadvantage relative to their unicellular ancestor (that is, no direct benefits), which is compensated by the indirect benefits of being exposed to the oxygen-rich environment. In fact, when cells in the mat mutate back to their ancestral non-sticky phenotype—thereby avoiding the costs of group formation while still reaping the indirect benefits—they are able to outperform their sticky relatives[76]. Thus, this experiment provides an example of the emergence of multicellular groups through indirect benefits, in the absence of direct benefits. Although the multicellular mats are not yet part of a proper multicellular life cycle at this stage, they can become part of one, as it has been shown that a life cycle could naturally emerge in a metapopulation setting[77,79].

It is not yet clear whether there are any examples of organisms that indirectly benefit from being multicellular in their natural environment. However, indirect benefits offer a potential candidate explanation for multicellularity in some primitively multicellular organisms[80–87] where the benefits of multicellularity remain elusive. Many of these organisms navigate different environments throughout their life cycle[85–87], which provides the spatial heterogeneity required for indirect benefits to apply. If multicellularity were to indeed be only indirectly beneficial, that would also explain why these benefits are difficult to detect in a lab setting: multicellularity would not provide any advantage when solitary cells and multicellular groups are compared under the same conditions. Only an experimental set-up that incorporates spatial heterogeneity—as in the *Pseudomonas* example above—would allow potential indirect benefits to be revealed.

Even for extant complex multicellular organisms (for example, animals and plants), which today derive obvious direct benefits of multicellularity (for example, controlled cell differentiation), it is possible that indirect benefits played a role in a deep evolutionary past. At the origins of multicellularity, these lineages might have initially persisted through indirect—rather than direct—benefits, which could have provided a critical time window during which directly beneficial innovations such as cell differentiation could evolve.

Methods

Model description

Migration. Single cells and multicellular groups can migrate between the two different environments, A and B, but at possibly different rates (Fig. 1a). Single cells (whether belonging to the unicellular or multicellular strategy) migrate from environment A to environment B at rate $m_{1,AB}$ and from environment B to environment A at rate $m_{1,BA}$. Similarly, groups of size n migrate at rates $m_{n,AB}$ and $m_{n,BA}$. For instance, if A and B represent upper and lower layers of the water column, then $m_{n,AB}$ would increase with n (larger groups sink faster), while $m_{n,BA}$ would decrease with n.

Growth dynamics. The rate at which cells divide may depend on the environment and on the size of the group that they are in (Fig. 1b). Single cells (whether belonging to the unicellular or multicellular strategy) divide at a rate $r_{1,A}$ in environment A and at a rate $r_{1,B}$ in environment B. Cells that belong to groups of size n divide at rates $r_{n,A}$ and $r_{n,B}$. In our main analysis, we omit density-independent death, so that the intrinsic growth rate of cells is equal to their division rate. Our results remain qualitatively unchanged when we include density-independent death of solitary cells or whole groups (Supplementary Information section 2.6). To reflect the premise of no direct benefits, we assume that, for cells in groups of every size $n > 1$,

$$r_{n,A} < r_{1,A} \text{ and } r_{n,B} < r_{1,B}.$$

Thus, we assume that in both environments single cells have a higher intrinsic growth rate than cells in groups of any size.

Competition. Groups and single cells die from competition with others in the same environment (Fig. 1b). Specifically, cells and groups in environment A experience density-dependent death due to competition for the same resources at rate γT_A, where T_A is the total density of cells in environment A and γ is the competition rate. Similarly, cells and groups in environment B experience density-dependent death at rate γT_B. This form of density-dependent death does not bring a selective advantage to any life cycle, unicellular or multicellular[88].

Life cycles. In the unicellular strategy, each cell division gives rise to a new single cell (Fig. 1c). For the multicellular strategy, we consider three qualitatively different types of multicellular life cycles that capture some of the diversity in reproduction modes across simple multicellular organisms[89]: producing a single unicellular propagule (for example, some bacteria[90–92]), dissolution into many propagules (for example, some green algae[93] and ichthyosporeans[94]) and fission into two groups of roughly equal size (for example, some choanoflagellates[95] and golden algae[96]). We assume that cells stay together after cell division until a critical group size is reached, upon which fragmentation occurs according to a specific fragmentation pattern[97]:

$N+1$: Once groups reach size $N+1$, they instantaneously split into a group of size N and a single-cell propagule.
$N \times 1$: Once groups reach size N, they instantaneously disintegrate into N single-cell propagules.
$N/2 + N/2$: Once groups reach size N, they instantaneously split into two groups of equal size. If N is odd, one of the fragments ends up with an extra cell (that is, one group with $(N+1)/2$ cells and another with $(N-1)/2$ cells).

Spatial distributions. To keep track of the emergent spatial distributions of solitary cells and multicellular groups, we define q_A as the fraction of ancestral solitary cells that inhabit environment A at steady state; the remaining fraction $q_B = 1 - q_A$ inhabits environment B. Similarly, we denote by $p_{n,A}$ the fraction of groups of size $n \geq 1$ in environment A at steady state; the remaining fraction $p_{n,B} = 1 - p_{n,A}$ of groups of size n inhabits environment B. In particular, $p_{1,A}$ and $p_{1,B}$ describe the spatial distribution of single cells belonging to the multicellular strategy. Even though these cells are subject to the same migration rates as the ancestral solitary cells, they may nonetheless differ in their spatial distribution because of where they are produced. In general, the spatial distributions emerge from the interplay between migration, reproduction and competition. But, when migration occurs on a much faster timescale than reproduction and competition, the spatial distributions are entirely determined (Supplementary Information section 2.5) by the migration rates as

$$q_A = p_{1,A} = \frac{m_{1,BA}}{m_{1,AB} + m_{1,BA}} \tag{5}$$

and

$$p_{n,A} = \frac{m_{n,BA}}{m_{n,AB} + m_{n,BA}}. \tag{6}$$

Model equations

Here we present the model equations for the competition between a multicellular mutant with life cycle $N+1$ and the unicellular ancestor. The models for the $N\times 1$ and $N/2+N/2$ life cycles can be found in the Supplementary Appendix.

We denote the time-dependent densities of ancestral single cells in environments A and B by y_A and y_B, respectively. Furthermore, $x_{n,A}$ is the time-dependent density of mutant groups of size n in environment A and $x_{n,B}$ in environment B. The total time-dependent density of cells in environment A becomes

$$T_A = y_A + x_{1,A} + 2x_{2,A} + 3x_{3,A} + \ldots \tag{7}$$

and similarly for T_B. The population dynamics in environment A are therefore given by

$$\frac{\mathrm{d}y_A}{\mathrm{d}t} = r_{1,A}y_A - \gamma T_A y_A - m_{1,AB}y_A + m_{1,BA}y_B \tag{8}$$

for the unicellular ancestor and by

$$\frac{\mathrm{d}x_{1,A}}{\mathrm{d}t} = Nr_{N,A}x_{N,A} - r_{1,A}x_{1,A} - \gamma T_A x_{1,A} - m_{1,AB}x_{1,A} + m_{1,BA}x_{1,B}, \tag{9}$$

$$\begin{aligned}\frac{\mathrm{d}x_{n,A}}{\mathrm{d}t} &= (n-1)r_{n-1,A}x_{n-1,A} - nr_{n,A}x_{n,A} - \gamma T_A x_{n,A}\\ &\quad - m_{n,AB}x_{n,A} + m_{n,BA}x_{n,B}\ (\text{where } 1<n<N),\end{aligned} \tag{10}$$

$$\frac{\mathrm{d}x_{N,A}}{\mathrm{d}t} = (N-1)r_{N-1,A}x_{N-1,A} - \gamma T_A x_{N,A} - m_{N,AB}x_{N,A} + m_{N,BA}x_{N,B} \tag{11}$$

for the multicellular mutant. The equations for environment B are analogous. The terms γT_A and γT_B reflect the competition-driven density-dependent mortality in the two environments. For more details, see Supplementary Information section 1.

Condition for the invasion of a multicellular mutant

We show in Supplementary Information section 2.3 that a necessary and sufficient condition for the $N+1$ life cycle to invade the unicellular ancestor is

$$N!\frac{R_N}{C_N}\prod_{n=1}^{N-1}\frac{1}{n+\frac{C_n}{R_n}} > 1. \tag{12}$$

The left side of (12) equals the basic reproduction number of an $N+1$ life cycle: the expected number of single-cell propagules generated by one instantiation of the life cycle. For the $2+1$ life cycle, condition (12) becomes

$$2\frac{R_2}{C_2}\frac{1}{1+\frac{C_1}{R_1}} > 1, \tag{13}$$

which can be rearranged to obtain (3).

Invasion experiments with random parameters

For each panel in Fig. 2, we first fixed the total migration rate $M = m_{1,AB} + m_{1,BA} + m_{2,AB} + m_{2,BA}$ and the total reproduction rate $R = r_{1,A} + r_{1,B} + r_{2,A} + r_{2,B}$. We set $R = 1$ and used $M = 0.02$ for slow migration, $M = 1$ for intermediate migration and $M = 50$ for fast migration. Then, for each of these scenarios, we performed 10^4 simulations with randomly sampled parameters. We randomly sampled migration rates $m_{1,AB}, m_{1,BA}, m_{2,AB}$ and $m_{2,BA}$ with sum M by setting

$$m_{1,AB} = \frac{u_1}{\sum_{i=1}^4 u_i}M,\ m_{1,BA} = \frac{u_2}{\sum_{i=1}^4 u_i}M,\ m_{2,AB} = \frac{u_3}{\sum_{i=1}^4 u_i}M,\ m_{2,BA} = \frac{u_4}{\sum_{i=1}^4 u_i}M, \tag{14}$$

with $u_i \sim \mathrm{U}(0,1)$ uniformly distributed for $i = 1, 2, 3, 4$. We used a similar approach to randomly sample growth rates $r_{1,A}$, $r_{1,B}$, $r_{2,A}$ and $r_{2,B}$ with sum R. To impose the premise of no direct benefits, we re-sampled the growth rates until they satisfied $r_{1,A} > r_{2,A}$ and $r_{1,B} > r_{2,B}$. Every simulation had the same rate of competition $\gamma = 1$.

After parameters were sampled, we evaluated the steady state of the unicellular ancestor in isolation (y_A^* and y_B^*) by numerically simulating (8) until $t = 10^7$ (there is always a unique stable equilibrium; Supplementary Information section 2.1). With the unicellular ancestor's population density at steady state (y_A^* and y_B^*), the spatial distribution of ancestral cells is evaluated as

$$q_A = \frac{y_A^*}{y_A^* + y_B^*},\ \text{and}\ q_B = \frac{y_B^*}{y_A^* + y_B^*}. \tag{15}$$

Then, at this steady state, we evaluated the Jacobian matrix $\mathbf{M}$ for the differential equations associated with the $2+1$ life cycle ((9) and (11) for $N = 2$). That is,

$$\mathbf{M} = \begin{pmatrix} -r_{1,A} - \gamma y_A^* - m_{1,AB} & 2r_{2,A} & m_{1,BA} & 0\\ r_{1,A} & -\gamma y_A^* - m_{2,AB} & 0 & m_{2,BA}\\ m_{1,AB} & 0 & -r_{1,B} - \gamma y_B^* - m_{1,BA} & 2r_{2,B}\\ 0 & m_{2,AB} & r_{1,B} & -\gamma y_B^* - m_{2,BA} \end{pmatrix}, \tag{16}$$

with $\vec{x} = (x_{1,A}, x_{2,A}, x_{1,B}, x_{2,B})$. From the dominant eigenvector $\vec{v} = (v_{1,A}, v_{2,A}, v_{1,B}, v_{2,B})$, associated with the dominant eigenvalue λ, we obtain the spatial distribution of one-cell groups ($p_{1,A}$ and $p_{1,B}$) and two-cell groups ($p_{2,A}$ and $p_{2,B}$) during the invasion from rare. The expressions are given by

$$p_{1,A} = \frac{v_{1,A}}{v_{1,A}+v_{1,B}},\ p_{1,B} = \frac{v_{1,B}}{v_{1,A}+v_{1,B}},\ p_{2,A} = \frac{v_{2,A}}{v_{2,A}+v_{2,B}}\ \text{and}\ p_{2,B} = \frac{v_{2,B}}{v_{2,A}+v_{2,B}}; \tag{17}$$

see Supplementary Information section 2.2 for more details. Then, the values of R_1, R_2, C_1 and C_2 were calculated using (1) and (2).

The evolutionary outcome for each set of parameters was determined by numerically simulating the invasion of the $2+1$ life cycle into a resident unicellular population. First, the unicellular ancestor was simulated in isolation (equation (8)). We then introduced 10^{-4} single cells of the $2+1$ life cycle into each environment and simulated the full system using equations (8)–(11). Both simulations were run until $t = 10^7$, a duration considered sufficient to ensure that the system had reached steady state. We classified the ecological outcome as dominance when either the unicellular or multicellular total cell population (summed across both environments) fell below 10^{-6}, a threshold small enough to consider the corresponding population displaced. Otherwise, the outcome was classified as coexistence. Points were further categorized as stable equilibria when, over the last 10^3 time steps, the maximum variation of every variable in equations (8)–(11) was below 10^{-6}; otherwise, the outcome would be classified as oscillatory. No oscillations were observed.

The Proterozoic Ocean example

We assume that single cells are buoyant and inhabit the upper layer of the water column (environment A). Groups below a critical size N_S are also buoyant and stay in the upper layer. Once the critical size is reached, groups instantly sink to a lower layer (environment B). In other words, the spatial distribution of groups of any given size n is

$$p_{n,A} = \begin{cases} 1 \text{ if } n < N_S; \\ 0 \text{ if } n \geq N_S, \end{cases} \quad \text{and} \quad p_{n,B} = \begin{cases} 0 \text{ if } n < N_S; \\ 1 \text{ if } n \geq N_S. \end{cases} \tag{18}$$

In the upper layer of the water column, single cells and cells in small multicellular groups perform respiration and divide at high rates (r_o); after a critical group size N_U, we assume that oxygen cannot diffuse deeper into the multicellular body, and any cells past the critical size are limited to doing fermentation with a lower division rate r_f. Thus, the growth rates in the upper layer are given by

$$r_{n,A} = \begin{cases} r_o & \text{if } n \leq N_U; \\ \frac{N_U \cdot r_o + (n - N_U) \cdot r_f}{n} & \text{if } n > N_U. \end{cases} \tag{19}$$

In the lower layer, diffusion limitation can occur at even smaller group sizes. Thus, the maximal number of respiring cells in each group is reduced from N_U to $N_L \leq N_U$. The growth rates in the lower layer are

$$r_{n,B} = \begin{cases} r_o & \text{if } n \leq N_L; \\ \frac{N_L \cdot r_o + (n - N_L) \cdot r_f}{n} & \text{if } n > N_L. \end{cases} \tag{20}$$

Dynamical equations are provided in Supplementary Information section 3.3.

Finally, we relax the assumption of perfect spatial segregation between the water layers by introducing the possibility of mixing: a proportion $0 \leq q_L \leq 0.5$ of single cells and groups below the sinking size N_S now inhabits the lower layer. More details are provided in Supplementary Information section 3.3.

Evolutionary simulations

To investigate the evolutionary dynamics of the Proterozoic Ocean example, we simulated the repeated introduction of rare mutants—that differ in their fragmentation size—in a resident community until an ESC (that is, a community that cannot be invaded by any life cycle not already present) was reached. Here we present the set-up and the procedure for our simulations. Detailed information on the evolutionary simulations is provided in Supplementary Information section 3.4.

Simulation set-up. The maximum fragmentation size allowed in our simulations is 121. Only one life cycle type ($N+1$, $N \times 1$ or $N/2 + N/2$) is allowed per simulation. Mutations are assumed to be global (that is, life cycles with fragmentation size M can produce mutants of any other fragmentation size $2 \leq M' \leq 121$ with the same probability); our results stay the same if the probability of mutations from M to M' decreases with $|M - M'|$). Even though the introduction of mutants is stochastic, all simulations with the same set of parameters eventually reach the same ESC.

Simulation procedure. Starting from a resident community exclusively composed by the unicellular ancestor (life cycle $1+1$), we randomly sample a life cycle $N+1$ ($1 \leq N \leq 120$) that is not present and is capable of invading (see Supplementary Information section 3.2 for the invasion conditions). Then, we simulate the invasion and let it reach steady state (a stable equilibrium is always reached; we never find oscillations). The invasion results in a new resident community (as some life cycles may have been competitively excluded), which could potentially be invaded again. If that is the case, we sample a new invader and repeat the process above. If the new resident community cannot be invaded by any life cycle that is not already present, we have reached an ESC, and the simulation is terminated. The specific details for the procedure above are detailed in Supplementary Information section 3.4.

Reporting summary

Further information on research design is available in the Nature Portfolio Reporting Summary linked to this article.

Data availability

The study is theoretical; no new empirical data were generated. All simulated data are available via Zenodo at https://doi.org/10.5281/zenodo.18749114 (ref. 98).

Code availability

All scripts needed to replicate the results presented here are available via Zenodo at https://doi.org/10.5281/zenodo.18749114 (ref. 98).

References

1. Bonner, J. T. The origins of multicellularity. *Integr. Biol. Issues News Rev.* **1**, 27–36 (1998).
2. Niklas, K. J. & Newman, S. A. The many roads to and from multicellularity. *J. Exp. Bot.* **71**, 3247–3253 (2020).
3. Herron, M. D., Conlin, P. L. and Ratcliff, W. C. *The Evolution of Multicellularity* (CRC, 2022).
4. Brunet, T. & King, N. The origin of animal multicellularity and cell differentiation. *Dev. Cell* **43**, 124–140 (2017).
5. Bonner, J. T. *First Signals: The Evolution of Multicellular Development* (Princeton Univ. Press, 2009).
6. Bonner, J. T. *The Evolution of Complexity by Means of Natural Selection* (Princeton Univ. Press, 1988).
7. Bowles, A. M., Williamson, C. J., Williams, T. A., Lenton, T. M. & Donoghue, P. C. The origin and early evolution of plants. *Trends Plant Sci.* **28**, 312–329 (2023).
8. Anbar, A. D. & Knoll, A. H. Proterozoic ocean chemistry and evolution: a bioinorganic bridge?. *Science* **297**, 1137–1142 (2002).
9. Mills, D. B. & Canfield, D. E. Oxygen and animal evolution: did a rise of atmospheric oxygen 'trigger' the origin of animals?. *BioEssays* **36**, 1145–1155 (2014).
10. Lyons, T. W. et al. Co-evolution of early earth environments and microbial life. *Nat. Rev. Microbiol.* **22**, 572–586 (2024).
11. Knoll, A. H., Javaux, E. J., Hewitt, D. & Cohen, P. Eukaryotic organisms in proterozoic oceans. *Phil. Trans. R. Soc. B* **361**, 1023–1038 (2006).
12. Donoghue, P. C. & Clark, J. W. Plant evolution: streptophyte multicellularity, ecology, and the acclimatisation of plants to life on land. *Curr. Biol.* **34**, R86–R89 (2024).
13. Bowles, A. M., Williamson, C. J., Williams, T. A. & Donoghue, P. C. Cryogenian origins of multicellularity in Archaeplastida. *Genome Biol. Evol.* **16**, evae026 (2024).
14. Carlisle, E., Yin, Z., Pisani, D. & Donoghue, P. C. Ediacaran origin and Ediacaran-Cambrian diversification of metazoa. *Sci. Adv.* **10**, eadp7161 (2024).
15. Bozdag, G. O., Libby, E., Pineau, R., Reinhard, C. T. & Ratcliff, W. C. Oxygen suppression of macroscopic multicellularity. *Nat. Commun.* **12**, 2838 (2021).
16. Lürling, M. & Van Donk, E. Grazer-induced colony formation in scenedesmus: are there costs to being colonial?. *Oikos* **88**, 111–118 (2000).
17. Raff, R. A. & Raff, E. C. Respiratory mechanisms and the metazoan fossil record. *Nature* **228**, 1003–1005 (1970).
18. Boyd, M., Rosenzweig, F. & Herron, M. D. Analysis of motility in multicellular *Chlamydomonas reinhardtii* evolved under predation. *PLoS ONE* **13**, e0192184 (2018).
19. Roper, M., Dayel, M. J., Pepper, R. E. & Koehl, M. Cooperatively generated stresslet flows supply fresh fluid to multicellular choanoflagellate colonies. *Phys. Rev. Lett.* **110**, 228104 (2013).
20. Koehl, M. Selective factors in the evolution of multicellularity in choanoflagellates. *J. Exp. Zool. B* **336**, 315–326 (2021).
21. Dudin, O., Wielgoss, S., New, A. M. & Ruiz-Trillo, I. Regulation of sedimentation rate shapes the evolution of multicellularity in a close unicellular relative of animals. *PLoS Biol.* **20**, e3001551 (2022).

22. Ratcliff, W. C., Denison, R. F., Borrello, M. & Travisano, M. Experimental evolution of multicellularity. *Proc. Natl Acad. Sci. USA* **109**, 1595–1600 (2012).
23. Tong, K., Bozdag, G. O. & Ratcliff, W. C. Selective drivers of simple multicellularity. *Curr. Opin. Microbiol.* **67**, 102141 (2022).
24. Kapsetaki, S. E. & West, S. A. The costs and benefits of multicellular group formation in algae. *Evolution* **73**, 1296–1308 (2019).
25. Stockey, R. G. et al. Sustained increases in atmospheric oxygen and marine productivity in the neoproterozoic and palaeozoic eras. *Nat. Geosci.* **17**, 667–674 (2024).
26. Canfield, D. E. A new model for proterozoic ocean chemistry. *Nature* **396**, 450–453 (1998).
27. Buss, L. W. *The Evolution of Individuality* (Princeton Univ. Press, 2014).
28. Herron, M. D. & Michod, R. E. Evolution of complexity in the volvocine algae: transitions in individuality through Darwin's eye. *Evolution* **62**, 436–451 (2008).
29. Sommer, U., Charalampous, E., Genitsaris, S. & Moustaka-Gouni, M. Benefits, costs and taxonomic distribution of marine phytoplankton body size. *J. Plankton Res.* **39**, 494–508 (2017).
30. Rebolleda-Gomez, M. & Travisano, M. The cost of being big: local competition, importance of dispersal, and experimental evolution of reversal to unicellularity. *Am. Nat.* **192**, 731–744 (2018).
31. Grosberg, R. K. & Strathmann, R. R. The evolution of multicellularity: a minor major transition?. *Annu. Rev. Ecol. Evol. Syst.* **38**, 621–654 (2007).
32. Varahan, S., Walvekar, A., Sinha, V., Krishna, S. & Laxman, S. Metabolic constraints drive self-organization of specialized cell groups. *Elife* **8**, e46735 (2019).
33. Schwartzman, J. A. et al. Bacterial growth in multicellular aggregates leads to the emergence of complex life cycles. *Curr. Biol.* **32**, 3059–3069 (2022).
34. Narayanasamy, N. et al. Metabolically driven flows enable exponential growth in macroscopic multicellular yeast. *Sci. Adv.* **11**, eadr6399 (2025).
35. Lurling, M. Phenotypic plasticity in the green algae *Desmodesmus* and *Scenedesmus* with special reference to the induction of defensive morphology. *Ann. Limnol. Int. J. Lim.* **39**, 85–101 (2003).
36. Nakov, T., Ashworth, M. & Theriot, E. C. Comparative analysis of the interaction between habitat and growth form in diatoms. *ISME J.* **9**, 246–255 (2015).
37. Kirkegaard, J. B., Marron, A. O. & Goldstein, R. E. Motility of colonial choanoflagellates and the statistics of aggregate random walkers. *Phys. Rev. Lett.* **116**, 038102 (2016).
38. Colizzi, E. S., Vroomans, R. M. & Merks, R. M. Evolution of multicellularity by collective integration of spatial information. *Elife* **9**, e56349 (2020).
39. Vroomans, R. M. & Colizzi, E. S. Evolution of selfish multicellularity collective organisation of individual spatio-temporal regulatory strategies. *BMC Ecol. Evol.* **23**, 35 (2023).
40. Butterfield, N. J. Modes of pre-ediacaran multicellularity. *Precambrian Res.* **173**, 201–211 (2009).
41. Mentel, M. & Martin, W. Energy metabolism among eukaryotic anaerobes in light of proterozoic ocean chemistry. *Phil. Trans. R. Soc. B* **363**, 2717–2729 (2008).
42. Müller, M. et al. Biochemistry and evolution of anaerobic energy metabolism in eukaryotes. *Microbiol. Mol. Biol. Rev.* **76**, 444–495 (2012).
43. Martin, W. & Müller, M. The hydrogen hypothesis for the first eukaryote. *Nature* **392**, 37–41 (1998).
44. Brunet, T. and King, N. The single-celled ancestors of animals: a history of hypotheses. in *The Evolution of Multicellularity* (Taylor & Francis, 2022).
45. Haeckel, E. & Wright, E. P. The gastraea-theory, the phylogenetic classification of the animal kingdom and the homology of the germ-lamellae. *J. Cell Sci.* **2**, 142–165 (1874).
46. Mikhailov, K. V. et al. The origin of metazoa: a transition from temporal to spatial cell differentiation. *BioEssays* **31**, 758–768 (2009).
47. Ratcliff, W. C., Herron, M. D., Howell, K., Pentz, J. T. & Travisano, M. Experimental evolution of an alternating uni-and multicellular life cycle in *Chlamydomonas reinhardtii*. *Nat. Commun.* **4**, 2742 (2013).
48. Bozdag, G. O. et al. De novo evolution of macroscopic multicellularity. *Nature* **617**, 747–754 (2023).
49. Eppley, R. W., Holmes, R. W. & Strickland, J. D. Sinking rates of marine phytoplankton measured with a fluorometer. *J. Exp. Mar. Biol. Ecol.* **1**, 191–208 (1967).
50. Smetacek, V. Role of sinking in diatom life-history cycles: ecological, evolutionary and geological significance. *Mar. Biol.* **84**, 239–251 (1985).
51. Beardall, J. et al. Allometry and stoichiometry of unicellular, colonial and multicellular phytoplankton. *New Phytol.* **181**, 295–309 (2009).
52. Chang, H. N. & Murray, M.-Y. Estimation of oxygen penetration depth in immobilized cells. *Appl. Microbiol. Biotechnol.* **29**, 107–112 (1988).
53. Wang, H. et al. Two-billion-year transitional oxygenation of the Earth's surface. *Nature* **645**, 665–671 (2025).
54. Kotil, S. E. & Vetsigian, K. Emergence of evolutionarily stable communities through eco-evolutionary tunnelling. *Nat. Ecol. Evol.* **2**, 1644–1653 (2018).
55. Gadgil, S., Nanjundiah, V. & Gadgil, M. On evolutionarily stable compositions of populations of interacting genotypes. *J. Theor. Biol.* **84**, 737–759 (1980).
56. Stanley, S. M. An ecological theory for the sudden origin of multicellular life in the late Precambrian. *Proc. Natl Acad. Sci. USA* **70**, 1486–1489 (1973).
57. Margulis, L., Walker, J. & Rambler, M. Reassessment of roles of oxygen and ultraviolet light in Precambrian evolution. *Nature* **264**, 620–624 (1976).
58. Knoll, A. Did emerging continents trigger metazoan evolution?. *Nature* **276**, 701–703 (1978).
59. Tang, S., Pichugin, Y. & Hammerschmidt, K. An environmentally induced multicellular life cycle of a unicellular cyanobacterium. *Curr. Biol.* **33**, 764–769 (2023).
60. Tarnita, C. E., Taubes, C. H. & Nowak, M. A. Evolutionary construction by staying together and coming together. *J. Theor. Biol.* **320**, 10–22 (2013).
61. Chesson, P. General theory of competitive coexistence in spatially-varying environments. *Theor. Popul. Biol.* **58**, 211–237 (2000).
62. Snyder, R. E. & Chesson, P. How the spatial scales of dispersal, competition, and environmental heterogeneity interact to affect coexistence. *Am. Nat.* **164**, 633–650 (2004).
63. Snyder, R. E. When does environmental variation most influence species coexistence?. *Theor. Ecol.* **1**, 129–139 (2008).
64. Usinowicz, J. & Levine, J. M. Species persistence under climate change: a geographical scale coexistence problem. *Ecol. Lett.* **21**, 1589–1603 (2018).
65. Levins, R. & Culver, D. Regional coexistence of species and competition between rare species. *Proc. Natl Acad. Sci. USA* **68**, 1246–1248 (1971).
66. Yu, D. W. & Wilson, H. B. The competition-colonization trade-off is dead; long live the competition-colonization trade-off. *Am. Nat.* **158**, 49–63 (2001).
67. Bolker, B. M. & Pacala, S. W. Spatial moment equations for plant competition: understanding spatial strategies and the advantages of short dispersal. *Am. Nat.* **153**, 575–602 (1999).
68. Loreau, M. & Ebenhoh, W. Competitive exclusion and coexistence of species with complex life cycles. *Theor. Popul. Biol.* **46**, 58–77 (1994).

69. Saltini, M., Vasconcelos, P. & Rueffler, C. Complex life cycles drive community assembly through immigration and adaptive diversification. *Ecol. Lett.* **26**, 1084–1094 (2023).
70. Moll, J. D. & Brown, J. S. Competition and coexistence with multiple life-history stages. *Am. Nat.* **171**, 839–843 (2008).
71. Miao, L., Yin, Z., Knoll, A. H., Qu, Y. & Zhu, M. 1.63-billion-year-old multicellular eukaryotes from the Chuanlinggou Formation in North China. *Sci. Adv.* **10**, eadk3208 (2024).
72. Han, T.-M. & Runnegar, B. Megascopic eukaryotic algae from the 2.1-billion-year-old Negaunee Iron-formation, Michigan. *Science* **257**, 232–235 (1992).
73. Agić, H., Moczydłowska, M. & Yin, L. Diversity of organic-walled microfossils from the early Mesoproterozoic Ruyang Group, North China Craton–a window into the early eukaryote evolution. *Precambrian Res.* **297**, 101–130 (2017).
74. Bengtson, S., Sallstedt, T., Belivanova, V. & Whitehouse, M. Three-dimensional preservation of cellular and subcellular structures suggests 1.6 billion-year-old crown-group red algae. *PLoS Biol.* **15**, e2000735 (2017).
75. Rainey, P. B. & Travisano, M. Adaptive radiation in a heterogeneous environment. *Nature* **394**, 69–72 (1998).
76. Rainey, P. B. & Rainey, K. Evolution of cooperation and conflict in experimental bacterial populations. *Nature* **425**, 72–74 (2003).
77. Hammerschmidt, K., Rose, C. J., Kerr, B. & Rainey, P. B. Life cycles, fitness decoupling and the evolution of multicellularity. *Nature* **515**, 75–79 (2014).
78. Rose, C. J., Hammerschmidt, K., Pichugin, Y. & Rainey, P. B. Meta-population structure and the evolutionary transition to multicellularity. *Ecol. Lett.* **23**, 1380–1390 (2020).
79. Black, A. J., Bourrat, P. & Rainey, P. B. Ecological scaffolding and the evolution of individuality. *Nat. Ecol. Evol.* **4**, 426–436 (2020).
80. Chin, N. E. et al. Formation of multicellular colonies by choanoflagellates increases susceptibility to capture by amoeboid predators. *J. Eukaryot. Microbiol.* **70**, e12961 (2023).
81. Kumler, W. E., Jorge, J., Kim, P. M., Iftekhar, N. & Koehl, M. Does formation of multicellular colonies by choanoflagellates affect their susceptibility to capture by passive protozoan predators?. *J. Eukaryot. Microbiol.* **67**, 555–565 (2020).
82. Sebé-Pedrós, A. et al. Regulated aggregative multicellularity in a close unicellular relative of metazoa. *eLife* **2**, e01287 (2013).
83. Suga, H. & Ruiz-Trillo, I. Development of ichthyosporeans sheds light on the origin of metazoan multicellularity. *Dev. Biol.* **377**, 284–292 (2013).
84. Sebé-Pedrós, A., Degnan, B. M. & Ruiz-Trillo, I. The origin of metazoa: a unicellular perspective. *Nat. Rev. Genet.* **18**, 498–512 (2017).
85. Datta, S. & Ratcliff, W. C. Illuminating a new path to multicellularity. *eLife* **11**, e83296 (2022).
86. Ros-Rocher, N. et al. Clonal-aggregative multicellularity tuned by salinity in a choanoflagellate. *Nature* **651**, 974–985 (2026).
87. Ferrer-Bonet, M. & Ruiz-Trillo, I. *Capsaspora owczarzaki*. *Curr. Biol.* **27**, R829–R830 (2017).
88. Ress, V., Traulsen, A. & Pichugin, Y. Eco-evolutionary dynamics of clonal multicellular life cycles. *eLife* **11**, e78822 (2022).
89. Pichugin, Y. & Traulsen, A. Evolution of multicellular life cycles under costly fragmentation. *PLoS Comput. Biol.* **16**, e1008406 (2020).
90. McDougald, D., Rice, S. A., Barraud, N., Steinberg, P. D. & Kjelleberg, S. Should we stay or should we go: mechanisms and ecological consequences for biofilm dispersal. *Nat. Rev. Microbiol.* **10**, 39–50 (2012).
91. Purevdorj-Gage, B., Costerton, W. & Stoodley, P. Phenotypic differentiation and seeding dispersal in non-mucoid and mucoid *Pseudomonas aeruginosa* biofilms. *Microbiology* **151**, 1569–1576 (2005).
92. Mizuno, K. et al. Novel multicellular prokaryote discovered next to an underground stream. *eLife* **11**, e71920 (2022).
93. Kirk, D. L. A twelve-step program for evolving multicellularity and a division of labor. *BioEssays* **27**, 299–310 (2005).
94. Olivetta, M., Bhickta, C., Chiaruttini, N., Burns, J. & Dudin, O. A multicellular developmental program in a close animal relative. *Nature* **635**, 382–389 (2024).
95. Dayel, M. J. et al. Cell differentiation and morphogenesis in the colony-forming choanoflagellate *Salpingoeca rosetta*. *Dev. Biol.* **357**, 73–82 (2011).
96. Goldstein, M., McLachlan, J. & Moore, J. Morphology and reproduction of *Synura lapponica* (Synurophyceae). *Phycologia* **44**, 566–571 (2005).
97. Pichugin, Y., Pena, J., Rainey, P. B. & Traulsen, A. Fragmentation modes and the evolution of life cycles. *PLoS Comput. Biol.* **13**, e1005860 (2017).
98. Jorge, D. Code for: Direct benefits are not necessary for the evolution of multicellularity. *Zenodo* https://doi.org/10.5281/zenodo.18749114 (2025).

Acknowledgements

We thank J. Levine, members of the Tarnita lab, and Princeton's Theory Tea community for helpful feedback. C.E.T. gratefully acknowledges support from a Guggenheim Fellowship.

Author contributions

All authors contributed equally to conceptual development, model design and paper writeup. D.J. and M.S. performed the simulations, analysed the results and conducted the mathematical analysis.

Competing interests

The authors declare no competing interests.

Additional information

Extended data is available for this paper at https://doi.org/10.1038/s41559-026-03044-y.

Supplementary information The online version contains supplementary material available at https://doi.org/10.1038/s41559-026-03044-y.

Correspondence and requests for materials should be addressed to Corina E. Tarnita.

Peer review information *Nature Ecology & Evolution* thanks Daniel Mills, Vidyanand Nanjundiah and the other, anonymous, reviewer(s) for their contribution to the peer review of this work. Peer reviewer reports are available.

https://doi.org/10.1038/s41559-026-03044-y

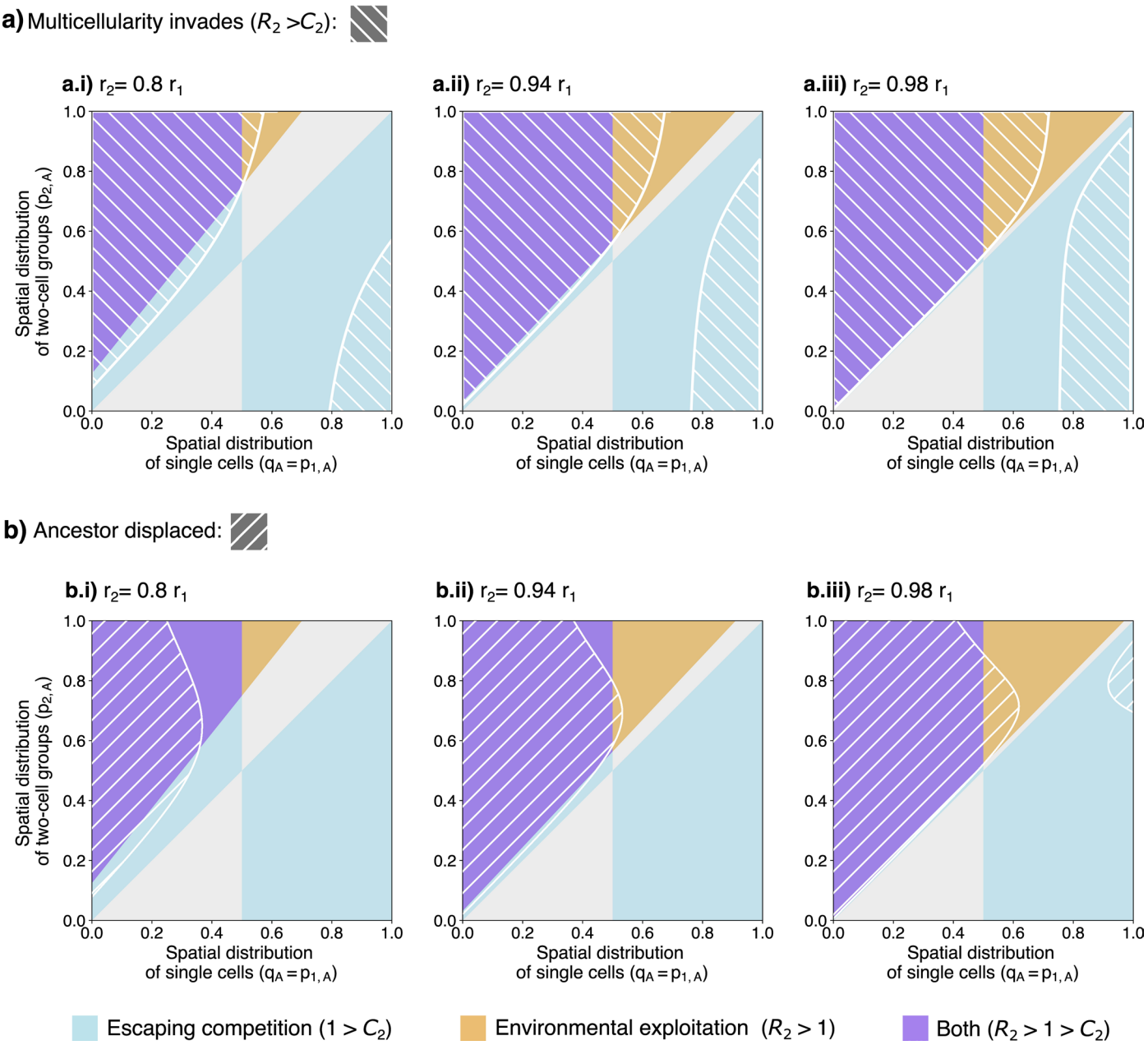

Extended Data Fig. 1 | Ecological outcomes of 2+1 invasion: coexistence or exclusion. Possible outcomes of the invasion of 2+1 in the fast migration limit, depending on the spatial distribution of solitary cells ($q_A = p_{1,A}$) and 2-cell groups ($p_{2,A}$). The space is colored based on the presence of indirect benefits: escaping competition (blue), environmental exploitation (orange), or both (purple). In (**a**), the white hatched region indicates where indirect benefits are strong enough to facilitate the invasion of multicellularity ($R_2 > C_2$). In (**b**), the white hatched region indicates where the multicellular mutant eventually displaces the unicellular ancestor. In each panel of (**a**) and (**b**), a different reduction in growth rates for cells in groups, relative to single cells, is assumed: (i) $r_2 = 0.8r_1$, (ii) $r_2 = 0.94r_1$, and (iii) $r_2 = 0.98r_1$. We set $r_{1,A} = 15$ and $r_{1,B} = 5$.

https://doi.org/10.1038/s41559-026-03044-y

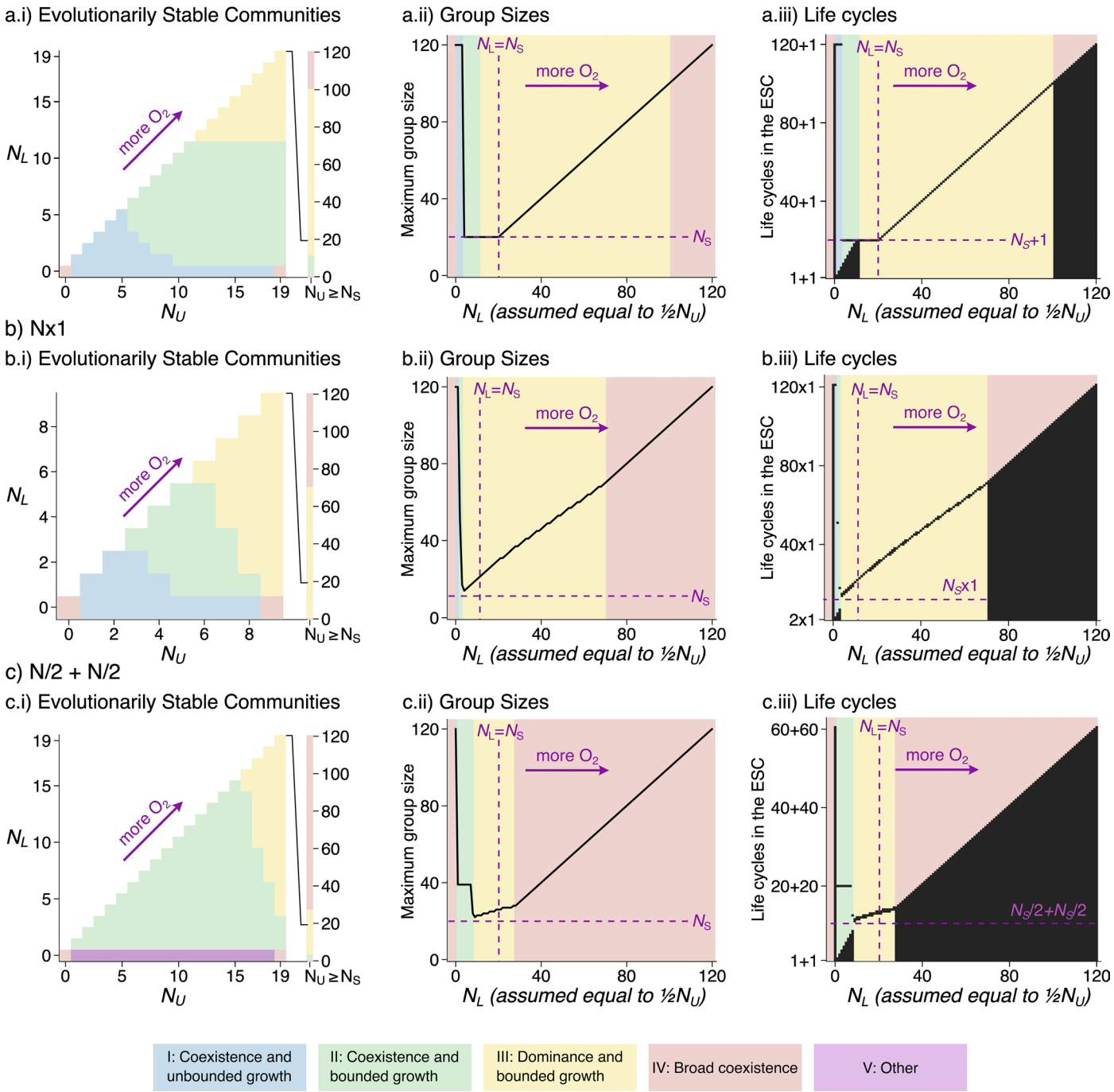

Extended Data Fig. 2 | Robustness analysis across life cycles: results for *N*+1, *N*×1 and *N*/2+*N*/2 life cycles. Evolutionarily stable communities (ESCs) for the different life cycle types: (**a**) $N+1$, (**b**) $N\times1$, (**c**) $N/2+N/2$. Colored regions indicate the different types of ESCs. For each life cycle type, we present: (i) ESC outcomes as a function of N_U and N_L (as in Fig. 5, when $N_U \geq N_S$, the value of N_U becomes irrelevant as all cells in the upper layer have access to oxygen); (ii) Maximum attained group sizes as a function of oxygen concentration, under the assumption that $N_U = 2N_L$; (iii) The full life cycle community present at each $N_U = 2N_L$ (each black square indicates the presence of the corresponding life cycle in the ESC). In (ii) and (iii), the colors in the background indicate the ESC reached for the given N_L. For the $N\times1$ and $N/2+N/2$ life cycles, the dominance ESC region is characterized by either a single dominant sinking life cycle or two adjacent sinking life cycles (two life cycles whose fragmentation sizes N and M differ by one cell, that is, $|N-M|=1$). Across different life cycles, the results remain qualitatively consistent. The only exception is a new ESC (purple) that appears for $N_L = 0$ in the $N/2+N/2$ life cycle, where all non-sinking life cycles that do not experience oxygen limitation coexist with all life cycles that never inhabit the lower layer (that is, $N+N$ with $N \geq N_S$). Simulations used $r_o = 6.8$, $r_f = 1$, and $\gamma = 1$. Life cycles $N+1$ and $N/2+N/2$ used $N_S = 20$ while $N\times1$ used $N_S = 10$. See Section S3.6 of the Supplementary Information for a brief discussion of these results.

https://doi.org/10.1038/s41559-026-03044-y

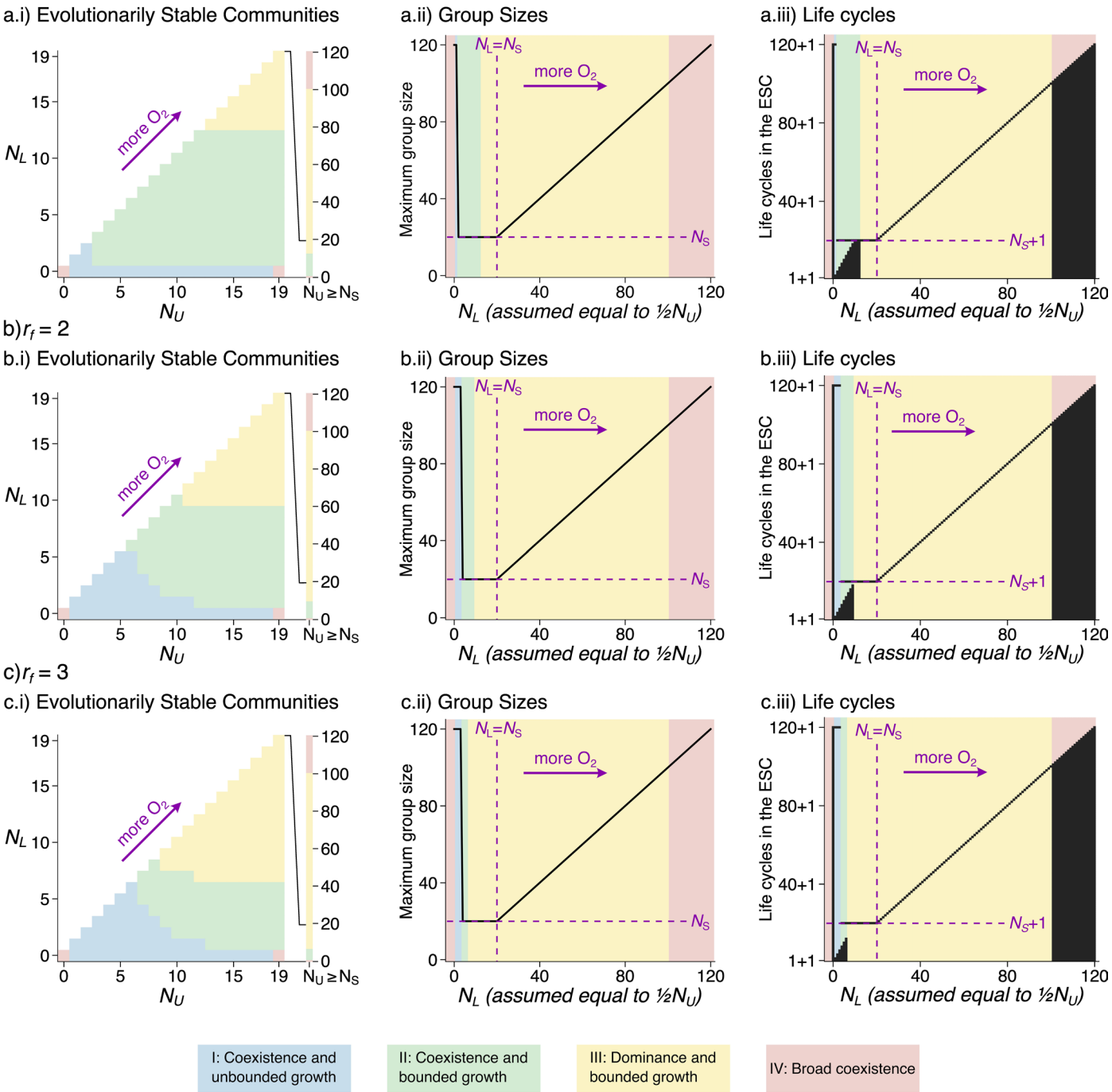

Extended Data Fig. 3 | Robustness analysis across fermentation growth rates: *N*+1 results for low r_f. Evolutionarily stable communities (ESCs) for different fermentation growth rates: (**a**) r_f=0.01, (**b**) r_f=2, (**c**) r_f=3. Colored regions indicate the different types of ESCs. For each fermentation rate, we present: (i) ESC outcomes as a function of N_U and N_L (as in Fig. 5, when $N_U \geq N_S$, the value of N_U becomes irrelevant as all cells in the upper layer have access to oxygen); (ii) Maximum attained group sizes as a function of oxygen concentration, under the assumption that $N_U = 2N_L$; (iii) The full life cycle community present at each $N_U = 2N_L$ (each black square indicates the presence of the corresponding life cycle in the ESC). In (ii) and (iii), the colors in the background indicate the ESC reached for the given N_L. Simulations used r_o=6.8, N_S=20, and γ=1. Across low fermentation growth rates ($0.01 \leq r_f \leq 3$), the results for N+1 remain qualitatively consistent relative to Fig. 5 (r_f=1). See Section S3.6 of the Supplementary Information for a brief discussion of these results.

https://doi.org/10.1038/s41559-026-03044-y

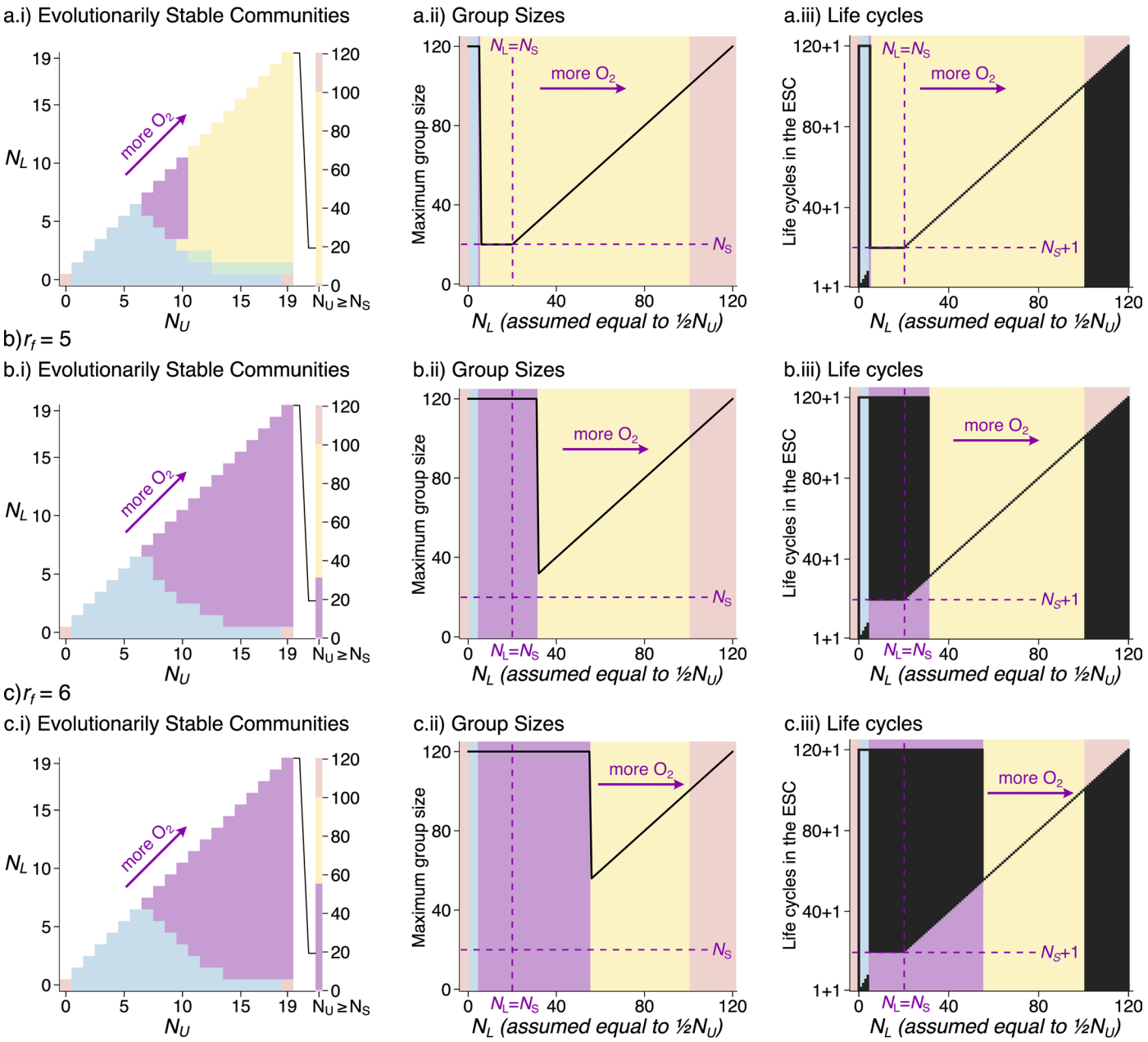

Extended Data Fig. 4 | Robustness analysis across fermentation growth rates: $N+1$ results for high r_f. Evolutionarily stable communities (ESCs) for different fermentation growth rates: (**a**) $r_f = 4$, (**b**) $r_f = 5$, (**c**) $r_f = 6$. Colored regions indicate the different types of ESCs. For each fermentation rate, we present: (i) ESC outcomes as a function of N_U and N_L (as in Fig. 5, when $N_U \geq N_S$, the value of N_U becomes irrelevant as all cells in the upper layer have access to oxygen); (ii) Maximum attained group sizes as a function of oxygen concentration, under the assumption that $N_U = 2N_L$; (iii) The full life cycle community present at each $N_U = 2N_L$ (each black square indicates the presence of the corresponding life cycle in the ESC). In (ii) and (iii), the colors in the background indicate the ESC reached for the given N_L. Simulations used $r_o = 6.8$, $N_S = 20$, and $\gamma = 1$. Across high fermentation growth rates ($4 \leq r_f \leq 6$), the results for $N+1$ remain qualitatively consistent, except when r_f becomes too high. For $r_f = 5$ (**b**) and $r_f = 6$ (**c**), we find a new evolutionary outcome (purple): non-sinking life cycles are displaced, and all sinking life cycles that grow past a threshold coexist neutrally (iii). In Section S4 of the Supplementary Information, we analytically show that the ESC regimes described in the main text, together with the additional regime highlighted above (purple), are the only possible ESCs for the $N+1$ life cycle. See Section S3.6 of the Supplementary Information for a brief discussion of these results.

https://doi.org/10.1038/s41559-026-03044-y

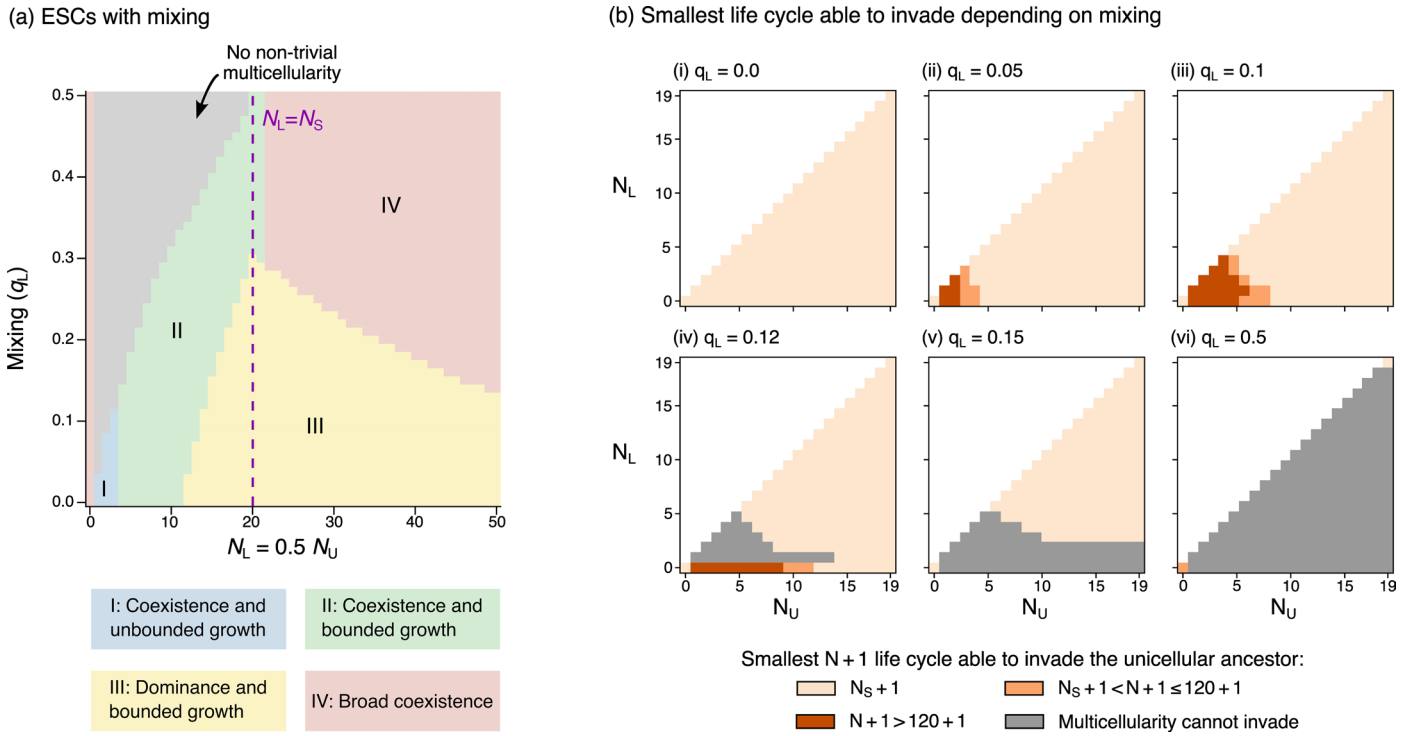

Extended Data Fig. 5 | Robustness analysis across different degrees of mixing. (**a**) ESC outcomes when there is some mixing and a proportion q_L of single cells and groups below size N_S inhabit the lower layer (see Section S3.6 of the Supplementary Information for a brief discussion of these results). In part of the gray region, evolving non-trivial multicellularity is impossible altogether; in the other part, it can only evolve for very high fragmentation sizes, not captured in our simulations. Thus, for the $N+1$ life cycle, we calculate the smallest fragmentation size able to invade the unicellular ancestor as a function of N_U and N_L, and across different mixing (q_L) values (**b**). To determine if multicellularity can invade, we first numerically evaluate Result S2.3 (see Section S2 of the Supplementary Information) for all $N+1$ life cycles up to fragmentation size 121. If none of these life cycles can invade but $\rho(N)$ is increasing with N for $N > N_S$ (and, therefore, $T_B^* > r_f/\gamma$), we know that eventually a very large life cycle ($N+1$ with $N > 120$; darkest orange in the figure) will invade (see Section S4.5 of the Supplementary Information).

nature portfolio

Corresponding author(s): Corina Tarnita

Last updated by author(s): Feb 23, 2026

Reporting Summary

Nature Portfolio wishes to improve the reproducibility of the work that we publish. This form provides structure for consistency and transparency in reporting. For further information on Nature Portfolio policies, see our Editorial Policies and the Editorial Policy Checklist.

Statistics

For all statistical analyses, confirm that the following items are present in the figure legend, table legend, main text, or Methods section.

n/a	Confirmed	
☐	☒	The exact sample size (*n*) for each experimental group/condition, given as a discrete number and unit of measurement
☒	☐	A statement on whether measurements were taken from distinct samples or whether the same sample was measured repeatedly
☒	☐	The statistical test(s) used AND whether they are one- or two-sided *Only common tests should be described solely by name; describe more complex techniques in the Methods section.*
☒	☐	A description of all covariates tested
☒	☐	A description of any assumptions or corrections, such as tests of normality and adjustment for multiple comparisons
☒	☐	A full description of the statistical parameters including central tendency (e.g. means) or other basic estimates (e.g. regression coefficient) AND variation (e.g. standard deviation) or associated estimates of uncertainty (e.g. confidence intervals)
☒	☐	For null hypothesis testing, the test statistic (e.g. *F*, *t*, *r*) with confidence intervals, effect sizes, degrees of freedom and *P* value noted *Give P values as exact values whenever suitable.*
☒	☐	For Bayesian analysis, information on the choice of priors and Markov chain Monte Carlo settings
☒	☐	For hierarchical and complex designs, identification of the appropriate level for tests and full reporting of outcomes
☒	☐	Estimates of effect sizes (e.g. Cohen's *d*, Pearson's *r*), indicating how they were calculated

Our web collection on statistics for biologists contains articles on many of the points above.

Software and code

Policy information about availability of computer code

Data collection	Custom Python and Julia code was used to run simulations. The code is a available at https://doi.org/10.5281/zenodo.18749114
Data analysis	Custom Python and Julia code was used to analyze the data.

For manuscripts utilizing custom algorithms or software that are central to the research but not yet described in published literature, software must be made available to editors and reviewers. We strongly encourage code deposition in a community repository (e.g. GitHub). See the Nature Portfolio guidelines for submitting code & software for further information.

Data

Policy information about availability of data

All manuscripts must include a data availability statement. This statement should provide the following information, where applicable:

- Accession codes, unique identifiers, or web links for publicly available datasets
- A description of any restrictions on data availability
- For clinical datasets or third party data, please ensure that the statement adheres to our policy

The study is theoretical; no new empirical data were generated. Our simulated data can be found at https://doi.org/10.5281/zenodo.18749114

Research involving human participants, their data, or biological material

Policy information about studies with human participants or human data. See also policy information about sex, gender (identity/presentation), and sexual orientation and race, ethnicity and racism.

Reporting on sex and gender	N/A
Reporting on race, ethnicity, or other socially relevant groupings	N/A
Population characteristics	N/A
Recruitment	N/A
Ethics oversight	N/A

Note that full information on the approval of the study protocol must also be provided in the manuscript.

Field-specific reporting

Please select the one below that is the best fit for your research. If you are not sure, read the appropriate sections before making your selection.

☐ Life sciences ☐ Behavioural & social sciences ☒ Ecological, evolutionary & environmental sciences

For a reference copy of the document with all sections, see nature.com/documents/nr-reporting-summary-flat.pdf

Ecological, evolutionary & environmental sciences study design

All studies must disclose on these points even when the disclosure is negative.

Study description	We investigated whether multicellularity could have evolved in the absense of direct benefits. We show that the answer is yes, as long as spatial heterogeneity is present. The study was conducted by the analysis of a mathematical model through analytical calculations and simulations implemented in Python and Julia.
Research sample	All data were generated by running simulations of the computational model.
Sampling strategy	For the analysis in Figure 2, we explored the parameter space by sampling 10,000 parameter sets per scenario (Fig2a, b, and c). For the analysis in Figure 5, multiple replicate simulations were run for each parameter combination (all replicates yielded the same result).
Data collection	All data were collected from the simulations.
Timing and spatial scale	Each simulation was run for at least 10,000,000 time steps. The spatial structure of the model includes two distinct environments and all simulated data were sampled and analyzed at this spatial scale.
Data exclusions	No data were excluded from the analyses.
Reproducibility	Not applicable as all data were generated using computer simulations.
Randomization	Not applicable as all data were generated using computer simulations.
Blinding	Blinding was not performed as the data were analyzed algorithmically rather than manually; results for each simulation were processed using the same computational pipeline.

Did the study involve field work? ☐ Yes ☒ No

Reporting for specific materials, systems and methods

We require information from authors about some types of materials, experimental systems and methods used in many studies. Here, indicate whether each material, system or method listed is relevant to your study. If you are not sure if a list item applies to your research, read the appropriate section before selecting a response.

Materials & experimental systems

n/a	Involved in the study
☒	☐ Antibodies
☒	☐ Eukaryotic cell lines
☒	☐ Palaeontology and archaeology
☒	☐ Animals and other organisms
☒	☐ Clinical data
☒	☐ Dual use research of concern
☒	☐ Plants

Methods

n/a	Involved in the study
☒	☐ ChIP-seq
☒	☐ Flow cytometry
☒	☐ MRI-based neuroimaging

Plants

Seed stocks	N/A
Novel plant genotypes	N/A
Authentication	N/A